

Assessment of the consistent second-order plate theory for isotropic plates from the perspective of the three-dimensional theory of elasticity

R. Kienzler*¹, M. Kashtalyan²

¹Bremen Institute of Mechanical Engineering (bime), University of Bremen, Department of Production Engineering, Am Biologischen Garten 2, 28359 Bremen, Germany

²Centre for Micro- and Nanomechanics (CEMINACS), School of Engineering, University of Aberdeen, Fraser Noble Building, Aberdeen AB24 3UE, Scotland UK

Keywords: consistent plate theory; isotropic plate; three-dimensional theory of elasticity; closed-form solution; Youngdahl's displacement potentials

Abstract

In this paper, the consistent second-order plate theory for isotropic plates is validated against the three-dimensional elasticity theory using a well-known benchmark problem of a simply-supported rectangular plate subjected to symmetric transverse sinusoidal loading. The choice of the benchmark problem is based on the fact that it allows for an exact three-dimensional elasticity solution to be derived in closed form. In the paper, two equivalent closed-form solutions are employed for validation purposes, one of which is specifically derived for this study. Once the equivalence of the two closed-form analytical solutions is established, they are expanded into a power-law series with respect to the non-dimensionalised plate thickness. This enables a direct term-by-term comparison with the consistent second-order plate theory solution and provides a valuable mechanism to validate the consistent plate theory in purely analytical form. The term-by-term comparison reveals that the first terms of the above power-law series coincide exactly with the expressions of the consistent second-order plate theory. In addition to the analytical validation, a parametric study is carried out with a view to establish the range of applicability of the consistent second-order plate theory in terms of the thickness-to-length ratio. It is demonstrated that the consistent plate theory can predict displacements and stresses in thick plates with very high degree of accuracy, such that even for very thick plates with thickness-to-length ratio of $1/2$, the deviation from the three-dimensional elasticity solution is less than 1%.

*Corresponding author

1. Introduction

Thin, moderately thin, and thick plate-like components are widely used in many engineering applications. For design and analysis of such components, two-dimensional theoretical constructions known as plate theories are usually employed which take advantage of the plate geometry and the fact that its thickness is (much) smaller than its in-plane dimensions. While exact three-dimensional elasticity solutions provide valuable benchmarks for validating specific plate theories, two-dimensional plate theories have a much wider range of applicability as they can be employed to analyse a greater variety of static and dynamic phenomena, plate geometries, loadings, and boundary conditions. Given that the development of plate theories began in the 19th century, the literature in this research area is incredibly rich and it still continues to grow, as evidenced by the recent publications (Brischetto, 2017; Candiotti et al. 2017; Karttunen et al., 2017; Repka et al., 2018; Wang et al., 2019), to name but a few.

Plate theories are inherently approximate in that they attempt to describe the actual three-dimensional solid by quantities that are defined on a surface. Derivation of a two-dimensional plate theory from a three-dimensional theory of elasticity generally follows one of three approaches. The first, *classical or engineering approach* starts with a set of kinematical a priori assumptions for the displacement distribution in thickness direction accompanied by additional assumptions concerning the stress distribution. Either transverse shear strains are neglected, or their influence is considered by the introduction of shear-correction factors. A historical survey on classical plate theories may be found in, e.g., Szabo, (1987). The mathematical justifications of the classical theories were provided only quite recently (cf., e.g., Friesecke et al., 2002 a, b) that state them to arise as a limit of the three-dimensional theory of elasticity when the thickness goes to zero. The proofs use the comparatively young method of Γ -convergence, which was developed by Giorgi (1975).

Following the second, *direct approach*, all quantities “live” on a Cosserat-type surface endowed with a set of deformable directors attached to each point of the plane. Despite of the mathematical elegance, the main drawback of this approach lies in the problem of establishing constitutive relations. Material parameters are identified by comparisons with a set of solutions of known test problems. The choice of the test problems has a crucial influence on the resulting theory. An excellent overview of the theories relying on the direct approach is given in Altenbach et al., (2010).

The third approach develops lower-dimensional theories from the three-dimensional theory of elasticity by means of *series expansion*. Here, we only mention three lines of work, which we consider as the most rigorous ones. At first, the *school initiated by Vekua* (1955, 1985) is mentioned, which is based on a displacement ansatz with truncated series expansions with respect to a basis of Legendre polynomials. Taking more series coefficients into account leads to more complex theories, so that a hierarchy of increasing complexity is established.

An estimate of the approximation error, however, is not available. Secondly, the so-called *restricted-type theory* for mixed plate-membrane problems was introduced by Steigmann (2008, 2012) and recently extended by Pruchnicki (2014). It combines established modelling approaches of Koiter (1966, 1970a) by arguments taken from contributions based on Γ -convergence. In general, the method of Γ -convergence, which is successfully applied for the mathematical justification of classical theories, is unlikely to be able to justify refined theories, since, as a limit analysis, it always derives the leading-order approximation whereas refined theories have to consider effects of different scales. Finally, we mention the so called *consistent approach* (or *uniform-approximation approach*), which originates from treatises by Naghdi (1963), Koiter (1970 b), Krätzig (1980) and Kienzler (1982) and will be used further within this paper. The refined theories are derived from the Euler-Lagrange equations of the truncated energy. It has been shown (Schneider et al., 2014) that the infinite two-dimensional PDE system corresponding to the untruncated elastic potential is equivalent to the three-dimensional equilibrium equations of linear elasticity and, secondly, (Schneider and Kienzler, 2015a, 2019) an a priori estimate of the approximation error is given that results from the truncated energy series.

In a series of papers (Kienzler, 2002; Kienzler, 2004; Kienzler and Schneider, 2012; Schneider et al., 2014), a hierarchy of consistent plate theories has been developed. The advantage of a consistent plate theory of any order of approximation is that ALL terms related to that approximation are retained in a consistent and logical manner, which leads to the most accurate representation of stresses and displacements within the chosen approximation and facilitates a better understanding of the underlying mechanical phenomena. It can be shown that in static problems, it is sufficient to use a second-order approximation because the characteristic in-plane measure of the plate coincides with the plate in-plane dimensions. In dynamic problems, a higher-order approximation might be required as the characteristic in-plane measure (e.g., the wavelength) might be much smaller than the plate dimensions.

Comparison of existing second-order plate theories with a consistent plate theory reveals for example that Reissner's plate theory (Reissner 1944, 1945) is consistent within a second-order approximation, while some theories, which claim to improve this theory by a so-called third-order shear theory (Reddy, 1984; Wang et al., 2000), are not (c.f., Schneider and Kienzler, 2015b; Kienzler and Schneider, 2017).

A consistent plate theory is the most rigorous way of constructing a two-dimensional approximation of a three-dimensional state of stress and displacement field in a solid. Assessing a consistent plate theory from the perspective of three-dimensional elasticity theory can provide a unique insight into its workings, however, such assessment has not been performed until now. A direct comparison of the consistent plate theory and the three-dimensional elasticity theory becomes possible thanks to recent development of a

method to construct the displacement and stress fields within a second-order consistent theory (Kienzler and Schneider, 2017).

In this paper, the consistent second-order plate theory for isotropic plates is validated against the three-dimensional elasticity theory using a well-known benchmark problem of a simply-supported rectangular plate subjected to symmetric transverse sinusoidal loading. The choice of the benchmark problem is based on the fact that this problem allows for an exact three-dimensional elasticity solution to be derived in closed form. In the paper, two equivalent closed-form solutions are used for validation purposes. The first closed-form exact analytical solution is adapted from the work of Saidi et al (2009), who reformulated Navier's equations for solving three-dimensional elasticity problems to make them applicable to thick plate analysis. In the work of Saidi et al (2009), the plate was subjected to transverse loading on the top face, with bottom face being free, therefore the solution had to be modified for the case of symmetric loading (and some misprints corrected along the way). The second closed-form exact analytical solution is developed specifically for validation purposes of this study using the displacement potential method and employing Youngdahl's displacement potentials (Youngdahl, 1969) for representation of stresses and displacements in the plate. Once the equivalence of the two closed-form analytical solutions is established, they are expanded into a power-law series with respect to the non-dimensionalised plate thickness. This enables a direct term-by-term comparison with the consistent second-order plate theory solution and provides a valuable mechanism to validate this theory in purely analytical form. The term-by-term comparison reveals that the first terms of the above power-law series coincide exactly with the expressions of the consistent second-order plate theory. In addition to such analytical validation, a parametric study is also carried out to establish the range of applicability of the consistent second-order plate theory in terms of the thickness-to-length ratio. It is demonstrated that the consistent plate theory can predict displacements and stresses in thick plates with very high accuracy, such that even for very thick plates with $h/a = 1/2$ the deviation from a three-dimensional solution is less than 1%.

The remainder of the paper is organised as follows. In Section 2, we formulate the problem statement and specify the necessary boundary conditions. In Section 3, we solve the boundary-value problem of Section 2 in the framework of the consistent second-order plate theory. In Section 4, we present two exact closed-form three-dimensional elasticity solutions – one adapted from the work of Saidi et al. (2009), another derived specifically for this study using the displacement potential method. We establish that the two solutions are equivalent and satisfy the uniqueness of solution requirement. In Section 5, the exact closed-form three-dimensional elasticity solution is expanded into a power series with respect to the normalised thickness parameter h/a . This is followed by a direct term-by-term comparison with the consistent plate theory solution of Section 3. In Section 6, a

parametric study is performed over a range of thickness-to-length ratios with the view to establish the range of applicability of the consistent second-order plate theory.

2. Problem statement

It is assumed that the mid-plane of the plate occupies a bounded domain $A \subset \mathbb{R}^2$ of the Cartesian (x_1, x_2) -plane, whereas the plate continuum extends by $\pm h/2$ in x_3 -direction. The loads q^- and q^+ are applied at the upper and lower faces, respectively, and point in x_3 -direction as indicated in Fig. 1.

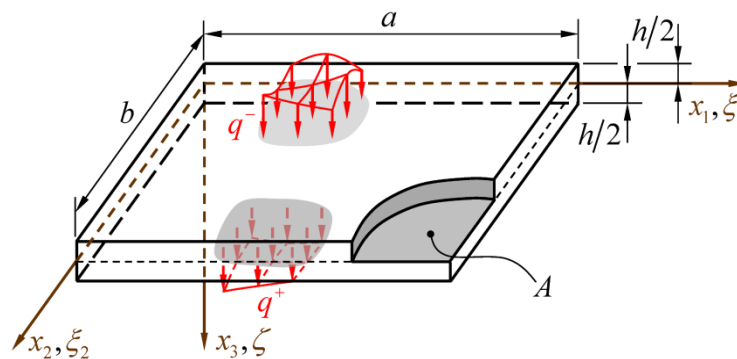


Fig. 1. Plate continuum

Volume forces in x_3 -direction, e.g., due to gravity, may also be applied, but will not be considered in the following. It may be mentioned that also in-plane loads with special symmetry properties may drive plate bending (Schneider & Kienzler, 2015a).

For the following, it is important that the applied forces q^+ at the lower face $x_3 = +h/2$ and the applied force q^- at the upper face $x_3 = -h/2$ are decomposed in symmetric and antisymmetric parts as depicted in Fig. 2

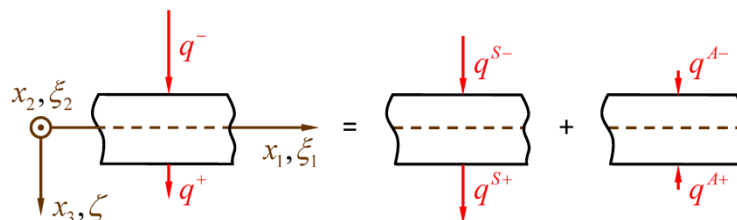


Fig. 2. Splitting of the loads applied to the plate faces $x_3 = \pm h/2$ into symmetric and antisymmetric parts

$$\begin{aligned}
q^{S+} = +q^{S-} &= \frac{1}{2}(q^+ + q^-), \\
q^{A+} = -q^{A-} &= \frac{1}{2}(q^+ - q^-).
\end{aligned}
\tag{2.1}$$

We combine the symmetric parts to the plate load q as

$$q = q^{S+} + q^{S-}, \tag{2.2}$$

whereas the antisymmetric part belongs to the in-plane disk problem (“squeezing” of the disk) not to be considered here.

Since we further restrict ourselves to isotropic materials, the plate and the disk problems are uncoupled (Schneider & Kienzler, 2017).

Within this paper, simply-supported rectangular ($a \times b$) plates are treated under a sinusoidal distribution of transverse loads

$$q = q_{mn} \sin \frac{m\pi x_1}{a} \sin \frac{n\pi x_2}{b}, \tag{2.3}$$

i.e.,

$$q^{S+} = q^{S-} = \frac{1}{2} q_{mn} \sin \frac{m\pi x_1}{a} \sin \frac{n\pi x_2}{b}. \tag{2.4}$$

The “wave numbers” m and n are positive integers and may be chosen arbitrarily. Thus (2.3) can be regarded as Fourier coefficient of a series expansion of a more general, even non-continuous load distribution. Since the governing equations are linear, the final solution of a specific loading case may be obtained by superposition.

For this restricted load and boundary conditions, not only closed form solutions of the partial differential equation (PDE) for various plate theories exist, but also a closed form solution of the PDE of the three-dimensional theory of linear elasticity is available. We elaborate both solutions and compare the results with each other.

To this end, we introduce dimensionless coordinates and notations

$$\begin{aligned}
\xi_1 &= \frac{x_1}{a}, \\
\xi_2 &= \frac{x_2}{a}, \quad \alpha \xi_2 = \frac{x_2}{b}, \\
\zeta &= \frac{x_3}{a},
\end{aligned}
\tag{2.5}$$

$$\alpha = \frac{a}{b}, \quad \gamma_{mn} = \sqrt{(m\pi)^2 + (n\pi\alpha)^2},$$

and define displacements, rotations, stresses and stress resultants in the usual way, cf. Fig. 3-5.

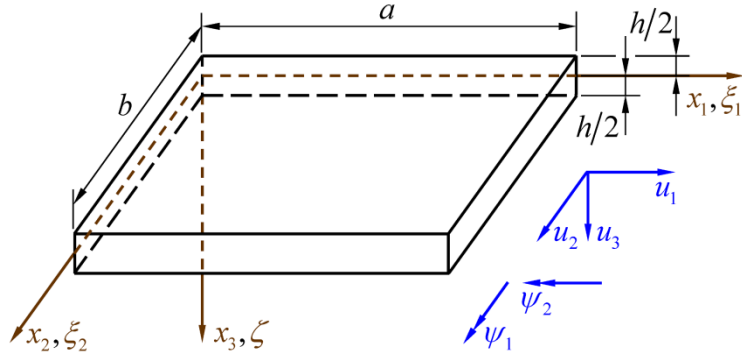


Fig. 3. Displacements and rotations

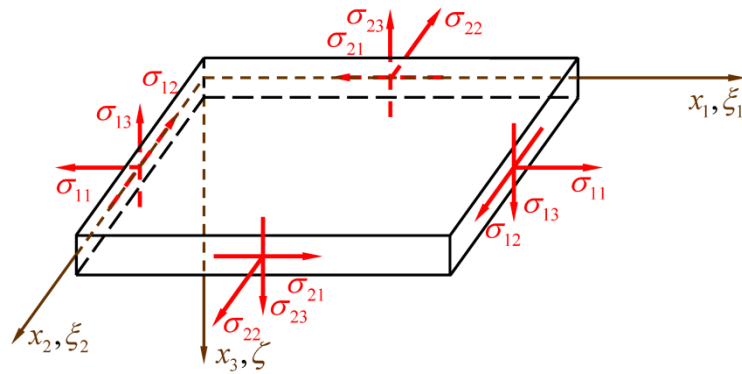


Fig. 4. Stresses at the plate continuum

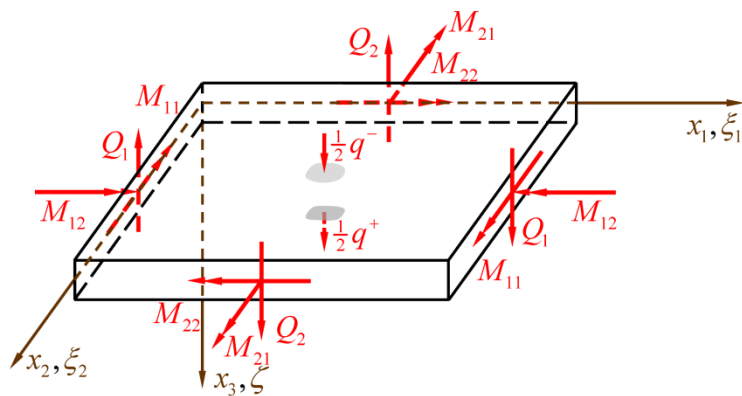


Fig. 5. Stress resultants and loads at the plate

In what follows, we will use the summation convention over repeated indices. Latin indices (i, j, k, \dots) have the range 1, 2, 3, whereas Greek indices ($\alpha, \beta, \gamma, \dots$) range over 1, 2.

The in-plane displacements are denoted by u_α [m] and the transverse displacement by u_3 [m]. A symbol in square brackets after a variable indicates the dimension of the variable, e.g., meter (m), Newton (N); non-dimensionalized variable: [1] In non-dimensionalised form, we introduce

$$u_3(\xi_1, \xi_2, 0) = aw(\xi_1, \xi_2), \quad (2.6)$$

where w [1] is not the non-dimensionalised transverse displacement of the middle surface but an energetic mean in Reissner's sense as

$$Q_\alpha w = \frac{a}{h} \int_{-\frac{h}{2a}}^{+\frac{h}{2a}} \sigma_{\alpha 3} u_3 d\zeta. \quad (2.7)$$

For details, cf., e.g., Kienzler and Schneider (2017) (w is denoted by w^K in that paper). Also the rotations ψ_α [1] are not understood as the linear part of u_α in thickness direction ($u_\alpha \neq a\psi_\alpha \zeta$) but are, again, energetic averages defined as

$$\frac{1}{a} M_{\alpha\beta} n_\alpha \psi_\beta = \frac{a}{n} \int_{-\frac{h}{2a}}^{+\frac{h}{2a}} \sigma_{\alpha\beta} u_\beta n_\alpha d\zeta. \quad (2.8)$$

$\sigma_{\alpha\beta}$ [MPa] are in-plane normal and shear stresses, $\sigma_{\alpha 3}$ [MPa] are transverse shear stresses and σ_{33} [MPa] is the normal stress in thickness direction. Q_α $\left[\frac{\text{N}}{\text{m}}\right]$ are the transverse shear stress resultants (forces per unit of length each), M_{11} and M_{22} $\left[\frac{\text{Nm}}{\text{m}}\right]$ are bending moments, $M_{12} = M_{21}$ $\left[\frac{\text{Nm}}{\text{m}}\right]$ are twisting moments (moments per unit of length each) and q $\left[\frac{\text{N}}{\text{m}^2}\right]$ is the applied transverse load per unit of area.

For simply supported plates, the boundary conditions read

$$\begin{aligned} \xi_1 = 0, 1 & : M_{11} = 0, & \psi_2 = 0, & u_3 = 0; \\ \alpha \xi_2 = 0, 1 & : M_{22} = 0, & \psi_1 = 0, & u_3 = 0; \\ \zeta = \pm \frac{h}{2a} & : \sigma_{33} = \pm \frac{1}{2} q, & \sigma_{31} = 0, & \sigma_{32} = 0. \end{aligned} \quad (2.9)$$

These boundary conditions are sometimes called “constraint” simply supported or “Klemmschneidenlagerung” in order to distinguish from the “unconstrained” simply supported or “free” supported, where instead of $\psi_2, M_{12} = 0$ is prescribed at $\xi_1 = 0, 1$ and instead of $\psi_1, M_{21} = 0$ is prescribed at $\alpha\xi_2 = 0, 1$.

Correspondently, when treating the problem within the framework of linear three-dimensional elasticity, we employ the boundary conditions

$$\begin{aligned} \xi_1 = 0, 1 & : \sigma_{11} = 0, & u_2 = 0, & u_3 = 0; \\ \alpha\xi_2 = 0, 1 & : \sigma_{22} = 0, & u_1 = 0, & u_3 = 0; \\ \zeta = \pm \frac{h}{2a} & : \sigma_{33} = \pm \frac{1}{2}q, & \sigma_{31} = 0, & \sigma_{32} = 0. \end{aligned} \quad (2.10)$$

Within any second-order plate theory, a quantity ψ appears

$$\psi = \varepsilon_{3\alpha\beta} \psi_{\beta,\alpha} = \psi_{2,1} - \psi_{1,2} \quad (2.11)$$

($\varepsilon_{3\alpha\beta}$ is the completely skew-symmetric permutation tensor, an index following a comma indicates differentiation with respect to the indicated non-dimensionalised variable, i.e., $(\cdot)_{,\alpha} = \partial(\cdot)/\partial\xi_\alpha$), which measures the deviation from the classical Kirchhoff-Love normal hypothesis $\psi_\alpha = -w_{,\alpha}$ and may therefore be regarded as a measure of the transverse-shear deformation. From Reissner’s theory (Reissner 1944, 1945) we know that ψ is a fast decaying function and describes edge effects, cf. Schneider et al. (2014), Kienzler and Schneider (2017), Schneider and Kienzler (2017). Due to the prescribed boundary conditions (2.6) it can be shown easily that ψ vanishes at all boundaries $\xi_1, \alpha\xi_2 = 0, 1$, and it may be concluded that ψ vanishes identically also within the plate

$$\psi(\xi_1, \xi_2) \equiv 0. \quad (2.11)$$

3. Consistent plate theory solution

In this section, we present all necessary equations of the consistent second-order approximation from Kienzler and Schneider (2017). Note that all quantities used here are indexed in Kienzler and Schneider (2017) by a capital K on the upper right-hand side of the generic symbol.

With the dimensionless plate parameter

$$c^2 = \frac{h^2}{12a^2} \quad (3.1)$$

the plate stiffness K

$$K = \frac{Eh^3}{12(1-\nu^2)}, \quad (3.2)$$

Poisson's ratio ν and the two-dimensional Laplace operator $\Delta(\cdot) = (\cdot)_{,\alpha\alpha}$, the plate differential equations are given as

$$\begin{aligned} K\Delta\Delta w &= a^3 \left(1 - \frac{6}{5} \frac{2-\nu}{1-\nu} c^2 \Delta \right) q + O(c^6), \\ c^2 \left(1 - \frac{6}{5} c^2 \Delta \right) \psi &= 0 + O(c^6). \end{aligned} \quad (3.3)$$

The discussion of these equations and the comparison with those of other authors are given in detail in Kienzler and Schneider (2017), where also further references can be found. An implication of the uniform-approximation technique is also the following equation

$$c^2 K \Delta \Delta w = c^2 a^3 q + O(c^6), \quad (3.4)$$

which will be used in the following. It may merely be mentioned that $q, \psi, c^2 \Delta \psi$ and $\frac{K}{a^2 h}$ are of order $O(c^2)$.

After solving (3.3) for w and ψ , the relation between the energetic means $w, \psi_{,\beta}$ and ψ follows to be

$$c^2 \psi_{,\beta} = -c^2 \left[\left(1 + \frac{12}{5} \frac{c^2}{1-\nu} \Delta \right) w_{,\beta} + \frac{6}{5} c^2 \varepsilon_{3\beta\gamma} \psi_{,\gamma} \right] + O(c^6), \quad (3.5)$$

the moments can be calculated from

$$\begin{aligned} M_{\alpha\beta} &= -\frac{K}{a} \left\{ \left(1 + \frac{12}{5(1-\nu)} c^2 \Delta \right) \left((1-\nu) w_{,\alpha\beta} + \nu w_{,\gamma\gamma} \delta_{\alpha\beta} \right) \right. \\ &\quad \left. + \frac{3}{5} (1-\nu) c^2 \left(\varepsilon_{3\alpha\gamma} \psi_{,\beta} + \varepsilon_{3\beta\gamma} \psi_{,\alpha} \right)_{,\gamma} \right\} \\ &\quad + \frac{6}{5} \frac{\nu}{1-\nu} c^2 a^2 q \delta_{\alpha\beta} + O(c^6), \end{aligned} \quad (3.6)$$

and two equivalent variants for the transverse-shear follow as

$$\begin{aligned}
Q_\beta &= -\frac{K}{a^2} \left\{ \left(1 + \frac{12}{5(1-\nu)} c^2 \Delta \right) \Delta w_{,\beta} + \frac{1}{2} (1-\nu) \varepsilon_{3\beta\gamma} \psi_{,\gamma} \right\} \\
&\quad + \frac{6}{5} \frac{\nu}{1-\nu} c^2 a q_{,\beta} + O(c^6), \\
Q_\beta &= -\frac{K}{a^2} \left\{ \Delta w_{,\beta} + \frac{1}{2} (1-\nu) \varepsilon_{3\beta\gamma} \psi_{,\gamma} \right\} - \frac{6}{5} \frac{2-\nu}{1-\nu} c^2 a q_{,\beta} + O(c^6).
\end{aligned} \tag{3.7}$$

The equilibrium equations written in stress resultants

$$\begin{aligned}
\frac{1}{a} Q_{\beta,\beta} &= -q, \\
\frac{1}{a} M_{\alpha\beta,\alpha} &= Q_\beta
\end{aligned} \tag{3.8}$$

are equivalent to (3.3), respectively. In addition, the boundary conditions are prescribed along the curve Γ with unit outward normal vector n_α enclosing the plate middle surface as

$$\begin{aligned}
M_{\alpha\beta} n_\alpha \Big|_\Gamma &= M_{\alpha\beta}^* n_\alpha \quad \text{or} \quad \psi_\beta \Big|_\Gamma = \psi_\beta^*, \\
Q_\alpha n_\alpha \Big|_\Gamma &= Q_\alpha^* n_\alpha \quad \text{or} \quad w \Big|_\Gamma = w^*,
\end{aligned} \tag{3.9}$$

where starred quantities are sufficiently smooth data given along Γ .

The displacement field calculated a posteriori is obtained as

$$\begin{aligned}
u_\alpha &= a\zeta \left\{ -w_{,\alpha} - \frac{1}{30} \frac{c}{1-\nu} \left[9(10-\nu) - 5(2-\nu) \frac{\zeta^2}{c^2} \right] \Delta w_{,\alpha} \right. \\
&\quad - c^4 \left[A_1 + \frac{1}{120} \frac{1}{(1-\nu)^2} \left(36(25-13\nu) - 6(15-12\nu+\nu^2) \frac{\zeta^2}{c^2} \right. \right. \\
&\quad \quad \left. \left. + (3-\nu)(1-\nu) \frac{\zeta^4}{c^4} \right) \right] \Delta \Delta w_{,\alpha} \\
&\quad + \frac{c^2}{6} \left(9 - \frac{\zeta^2}{c^2} \right) \varepsilon_{3\gamma\alpha} \psi_{,\gamma} \\
&\quad \left. + \frac{c^4}{120} \left(9 - 6 \frac{\zeta^2}{c^2} + \frac{\zeta^4}{c^4} \right) \varepsilon_{3\gamma\alpha} \Delta \psi_{,\beta} + O(c^6) \right\},
\end{aligned} \tag{3.10}$$

$$\begin{aligned}
u_3 = a \left\{ w - \frac{1}{10} \frac{vc^2}{1-\nu} \left(3 - 5 \frac{\zeta^2}{c^2} \right) \Delta w \right. \\
+ c^4 \left[A_1 + \frac{1}{120} \frac{1}{(1-\nu)^2} \left(18(5-\nu^2) \frac{\zeta^2}{c^2} - 5(1-\nu^2) \frac{\zeta^4}{c^4} \right) \right] \Delta \Delta w \\
+ c^6 \left[A_2 + \frac{1}{2} \frac{\nu}{1-\nu} \frac{\zeta^2}{c^2} A_1 + \frac{1}{720} \frac{1}{(1-\nu)^2} \left(54 \frac{25-13\nu}{1-\nu} \frac{\zeta^2}{c^2} \right. \right. \\
\left. \left. - 9(10-\nu-\nu^2) \frac{\zeta^4}{c^4} + (2+\nu)(1-\nu) \frac{\zeta^6}{c^6} \right) \Delta \Delta \Delta w \right] + O(c^8) \left. \right\}.
\end{aligned}$$

The two constants, which have no influence on the stress distribution within the consistent second-order theory, A_1 and A_2 , remain undetermined. They will be evaluated later when the equations will be compared with the exact three-dimensional solution. From the displacements, the stresses can readily be calculated as

$$\begin{aligned}
\sigma_{\alpha\beta} = \frac{E\zeta}{1-\nu^2} \left\{ -(1-\nu)w_{,\alpha\beta} - \nu\Delta w\delta_{\alpha\beta} \right. \\
- \frac{1}{30}c^2 \left[9(10-\nu)\Delta w_{,\alpha\beta} + 9\nu\frac{5-\nu}{1-\nu}\Delta\Delta w\delta_{\alpha\beta} \right. \\
\left. \left. - 5\frac{\zeta^2}{c^2} \left((2-\nu)\Delta w_{,\alpha\beta} + \nu\Delta\Delta w\delta_{\alpha\beta} \right) \right] \right. \\
\left. + \frac{1}{12}c^2(1-\nu) \left(9 - \frac{\zeta^2}{c^2} \right) \left(\varepsilon_{3\gamma\alpha}\psi_{,\beta} + \varepsilon_{3\gamma\beta}\psi_{,\alpha} \right)_{,\gamma} + O(c^4) \right\},
\end{aligned} \tag{3.11}$$

$$\begin{aligned}
\sigma_{33} = \frac{E\zeta}{1-\nu^2} \left\{ \frac{1}{6}c^2 \left(9 - \frac{\zeta^2}{c^2} \right) \Delta\Delta w \right. \\
\left. + \frac{1}{60}c^4 \left(9\frac{25-13\nu}{1-\nu} - 6\frac{\zeta^2}{c^2}\frac{5-3\nu}{1-\nu} + \frac{\zeta^4}{c^4} \right) \Delta\Delta\Delta w + O(c^6) \right\}, \\
\sigma_{\alpha 3} = \frac{E}{1-\nu^2} \frac{1}{2} \left(3 - \frac{\zeta^2}{c^2} \right) \left\{ -c^2\Delta w_{,\alpha} \right. \\
- \frac{1}{30}c^4 \left(3\frac{25-13\nu}{1-\nu} - 5\frac{\zeta^2}{c^2} \right) \Delta\Delta w_{,\alpha} \\
\left. + \frac{1}{120}c^2(1-\nu)\varepsilon_{3\gamma\alpha} \left(60\psi + c^2 \left(3 - 5\frac{\zeta^2}{c^2} \right) \Delta\psi \right)_{,\gamma} + O(c^6) \right\}.
\end{aligned}$$

Within the consistent second-order theory, this stress distribution satisfies the boundary conditions along the plate faces $\zeta = \pm h/(2a)$

$$\begin{aligned}\sigma_{\alpha 3}\Big|_{\pm\frac{h}{2a}} &= 0 + O(c^6), \\ \sigma_{33}\Big|_{\pm\frac{h}{2a}} &= \pm\frac{1}{2}q + O(c^6)\end{aligned}\tag{3.12}$$

and the local homogeneous equilibrium conditions

$$\begin{aligned}\sigma_{\beta\alpha,\beta} + \sigma_{3\alpha,3} &= \frac{E\xi}{1-\nu^2}(0 + O(c^4)), \\ \sigma_{\alpha 3,\alpha} + \sigma_{33,3} &= \frac{E}{1-\nu^2}(0 + O(c^6)).\end{aligned}\tag{3.13}$$

Of course, with the displacement fields (3.10), the in-plane stresses $\sigma_{\alpha\beta}$ can exactly be evaluated up to the order of $O(c^6)$, which will be done in the following for the special solution treated there. The in-plane equilibrium conditions (3.13₁), however, would not be approximated to the order $O(c^6)$. This would only be possible, if the transverse-shear stresses $\sigma_{\alpha 3}$ (3.11₃) would be approximated to the next higher order, what is not possible with the given displacement field.

Now, we turn our attention to the solution of the boundary-value problem stated in Section 2, i.e., the solution of (3.3) with (2.12), under the load (2.3) and the boundary conditions (2.9).

Guided by the load distribution (2.3) we employ the obvious ansatz

$$w = C \sin m\pi\xi_1 \sin n\pi\alpha\xi_2,\tag{3.14}$$

and insert (3.14) and (2.3) into (3.3) leading with (2.5₆) to

$$C = \frac{a^3 q_{mn}}{K\gamma_{mn}^4} \left[1 + c^2 \gamma_{mn}^2 \frac{6}{5} \left(\frac{2-\nu}{1-\nu} \right) \right].\tag{3.15}$$

Thus, the transverse displacement w is given by

$$Kw = a^3 \frac{q_{mn}}{\gamma_{mn}^4} \left[1 + \frac{6}{5} c^2 \gamma_{mn}^2 \left(\frac{2-\nu}{1-\nu} \right) \right] \sin m\pi\xi_1 \sin n\pi\alpha\xi_2 + O(c^6).\tag{3.16}$$

From (3.5), we calculate the rotations

$$c^2\psi_1 = -c^2 \frac{a^3 q_{mn}}{K\gamma_{mn}^4} (m\pi) \cos m\pi\xi_1 \sin n\pi\alpha\xi_2 \left\{ 1 - \frac{6}{5} c^2 \gamma_{mn}^2 \left(\frac{\nu}{1-\nu} \right) \right\} + O(c^6),\tag{3.17}$$

$$c^2\psi_2 = -c^2 \frac{a^3 q_{mn}}{K\gamma_{mn}^4} (n\pi\alpha) \sin m\pi\xi_1 \cos n\pi\alpha\xi_2 \left\{ 1 - \frac{6}{5} c^2 \gamma_{mn}^2 \left(\frac{\nu}{1-\nu} \right) \right\} + O(c^6)$$

(with $\psi = \psi_{2,1} - \psi_{1,2} \equiv 0$). The stress resultants follow from (3.6) as

$$M_{11} = \frac{q_{mn}}{\gamma_{mn}^4} a^2 \sin m\pi\xi_1 \sin n\pi\alpha\xi_2 \left\{ [(m\pi)^2 + \nu(n\pi\alpha)^2] \left[1 - \frac{6}{5} \left(\frac{\nu}{1-\nu} \right) c^2 \gamma_{mn}^2 \right] + \frac{6}{5} \frac{\nu c^2}{1-\nu} \right\} + O(c^6),$$

$$M_{22} = \frac{q_{mn}}{\gamma_{mn}^4} a^2 \sin m\pi\xi_1 \sin n\pi\alpha\xi_2 \left\{ [(n\pi\alpha)^2 + \nu(m\pi)^2] \left[1 - \frac{6}{5} \left(\frac{\nu}{1-\nu} \right) c^2 \gamma_{mn}^2 \right] + \frac{6}{5} \frac{\nu c^2}{1-\nu} \right\} + O(c^6),$$
(3.18)

$$M_{12} = -\frac{q_{mn}}{\gamma_{mn}^4} a^2 (1-\nu)(m\pi)(n\pi\alpha) \cos m\pi\xi_1 \cos n\pi\alpha\xi_2 \left\{ 1 - \frac{6}{5} \left(\frac{\nu}{1-\nu} \right) c^2 \gamma_{mn}^2 \right\} + O(c^6),$$

and from (3.7)

$$Q_1 = \frac{q_{mn} a (m\pi)}{\gamma_{mn}^2} \cos m\pi\xi_1 \sin n\pi\alpha\xi_2,$$

$$Q_2 = \frac{q_{mn} a (n\pi\alpha)}{\gamma_{mn}^2} \sin m\pi\xi_1 \cos n\pi\alpha\xi_2.$$
(3.19)

The boundary conditions (2.9) and the equilibrium conditions (3.8) are satisfied identically. Thus (3.16) is the exact analytical solution of our plate boundary-value problem.

Next, we calculate the displacements u_j from (3.10) and find

$$u_1 = \frac{a^4 q_{mn}}{K\gamma_{mn}^4} (m\pi) \zeta \cos m\pi\xi_1 \sin n\pi\alpha\xi_2 \left\{ -1 + c^2 \gamma_{mn}^2 \left[\frac{3}{10} \frac{2+3\nu}{1-\nu} - \frac{1}{6} \frac{2-\nu}{1-\nu} \frac{\zeta^2}{c^2} \right] \right. \\ \left. - c^4 \gamma_{mn}^4 \left[A_1 + \frac{3}{50} \frac{5+7\nu-6\nu^2}{(1-\nu)^2} + \frac{1}{20} \frac{1-3\nu}{1-\nu} \frac{\zeta^2}{c^2} + \frac{1}{120} \frac{3-\nu}{1-\nu} \frac{\zeta^4}{c^4} \right] + O(c^6) \right\},$$

$$u_2 = \frac{a^4 q_{mn}}{K\gamma_{mn}^4} (n\pi\alpha) \zeta \sin m\pi\xi_1 \cos n\pi\alpha\xi_2 \left\{ -1 + c^2 \gamma_{mn}^2 \left[\frac{3}{10} \frac{2+3\nu}{1-\nu} - \frac{1}{6} \frac{2-\nu}{1-\nu} \frac{\zeta^2}{c^2} \right] \right. \\ \left. - c^4 \gamma_{mn}^4 \left[A_1 + \frac{3}{50} \frac{5+7\nu-6\nu^2}{(1-\nu)^2} + \frac{1}{20} \frac{1-3\nu}{1-\nu} \frac{\zeta^2}{c^2} + \frac{1}{120} \frac{3-\nu}{1-\nu} \frac{\zeta^4}{c^4} \right] + O(c^6) \right\},$$
(3.20)

$$\begin{aligned}
u_3 = & \frac{a^4 q_{mn}}{K \gamma_{mn}^4} \sin m\pi \xi_1 \sin n\pi \alpha \xi_2 \left\{ 1 + c^2 \gamma_{mn}^2 \left[\frac{3}{10} \frac{8-3\nu}{1-\nu} - \frac{1}{2} \frac{\nu}{1-\nu} \frac{\zeta^2}{c^2} \right] \right. \\
& + c^4 \gamma_{mn}^4 \left[A_1 + \frac{9}{25} \frac{\nu(2-\nu)}{(1-\nu)^2} + \frac{3}{20} \frac{5-3\nu}{1-\nu} \frac{\zeta^2}{c^2} - \frac{1}{24} \frac{1+\nu}{1-\nu} \frac{\zeta^4}{c^4} \right] \\
& + c^6 \gamma_{mn}^6 \left[-A_2 + \frac{6}{5} \frac{2-\nu}{1-\nu} A_1 \right. \\
& \left. - \left(\frac{1}{2} \frac{\nu}{1-\nu} A_1 + \frac{3}{200} \frac{5-5\nu+24\nu^2-12\nu^3}{(1-\nu)^3} \right) \frac{\zeta^2}{c^2} \right. \\
& \left. + \frac{1}{80} \frac{2-3\nu}{1-\nu} \frac{\zeta^4}{c^4} - \frac{1}{720} \frac{2+\nu}{1-\nu} \frac{\zeta^6}{c^6} \right] + O(c^8) \left. \right\}.
\end{aligned}$$

As mentioned above, the constants A_1 and A_2 are not determined by the consistent second order theory. Note, since $\zeta \sim \frac{h}{a}$, the in-plane displacements u_α are one order of magnitude smaller than the transverse displacement u_3 .

We calculate the stresses $\sigma_{\alpha\beta}$ by taking in addition to (3.11) also the terms of order $O(c^4)$ into account. This leads to

$$\begin{aligned}
\sigma_{11} = & \frac{a\zeta}{hc^2 \gamma_{mn}^4} q_{mn} \sin m\pi \xi_1 \sin n\pi \alpha \xi_2 \cdot \\
& \left\{ (m\pi)^2 + \nu(n\pi\alpha)^2 + c^2 \gamma_{mn}^2 \left[-\frac{3}{5} (m\pi)^2 + \frac{9}{10} \nu(n\pi\alpha)^2 + \left(\frac{1}{3} (m\pi)^2 + \frac{\nu}{6} (n\pi\alpha)^2 \right) \frac{\zeta^2}{c^2} \right] \right. \\
& + c^4 \gamma_{mn}^4 \left[A_1 \left((m\pi)^2 + \nu(n\pi\alpha)^2 \right) + \frac{3}{100} \left(\frac{10+9\nu-7\nu^2}{(1-\nu)^2} (m\pi)^2 + \nu \frac{5+19\nu-12\nu^2}{(1-\nu)^2} (n\pi\alpha)^2 \right) \right. \\
& \left. + \frac{1}{20} \left((m\pi)^2 + 3\nu(n\pi\alpha)^2 \right) \frac{\zeta^2}{c^2} + \frac{1}{120} \left(3(m\pi)^2 + \nu(n\pi\alpha)^2 \right) \frac{\zeta^4}{c^4} \right] + O(c^6) \left. \right\},
\end{aligned}$$

$$\begin{aligned}
\sigma_{22} = & \frac{a\zeta}{hc^2 \gamma_{mn}^4} q_{mn} \sin m\pi \xi_1 \sin n\pi \alpha \xi_2 \cdot \\
& \left\{ (n\pi\alpha)^2 + \nu(m\pi)^2 + c^2 \gamma_{mn}^2 \left[-\frac{3}{5} (n\pi\alpha)^2 + \frac{9}{10} \nu(m\pi)^2 + \left(\frac{1}{3} (n\pi\alpha)^2 + \frac{\nu}{6} (m\pi)^2 \right) \frac{\zeta^2}{c^2} \right] \right. \\
& + c^4 \gamma_{mn}^4 \left[A_1 \left((n\pi\alpha)^2 + \nu(m\pi)^2 \right) + \frac{3}{100} \left(\frac{10+9\nu-7\nu^2}{(1-\nu)^2} (n\pi\alpha)^2 + \nu \frac{5+19\nu-12\nu^2}{(1-\nu)^2} (m\pi)^2 \right) \right. \\
& \left. + \frac{1}{20} \left((n\pi\alpha)^2 + 3\nu(m\pi)^2 \right) \frac{\zeta^2}{c^2} + \frac{1}{120} \left(3(n\pi\alpha)^2 + \nu(m\pi)^2 \right) \frac{\zeta^4}{c^4} \right] + O(c^6) \left. \right\},
\end{aligned}$$

$$\begin{aligned}
\sigma_{12} = & \frac{a\zeta}{hc^2\gamma_{mn}^4} q_{mn} \cos m\pi\xi_1 \cos n\pi\xi_2 (m\pi)(n\pi\alpha) \\
& \left\{ -(1-\nu) + c^2\gamma_{mn}^2 \left[\frac{3}{10}(2+3\nu) - \frac{1}{6}(2-\nu)\frac{\zeta^2}{c^2} \right] \right. \\
& \left. - c^4\gamma_{mn}^4 \left[A_1(1-\nu) + \frac{3}{50} \frac{5+7\nu-6\nu^2}{1-\nu} + \frac{1}{20}(1-3\nu)\frac{\zeta^2}{c^2} + \frac{1}{120}(3-\nu)\frac{\zeta^4}{c^4} \right] + O(c^6) \right\},
\end{aligned} \tag{3.21}$$

$$\begin{aligned}
\sigma_{13} = & \frac{a}{2h\gamma_{mn}^2} q_{mn} (m\pi) \cos m\pi\xi_1 \sin n\pi\alpha\xi_2 \left(3 - \frac{\zeta^2}{c^2} \right) \cdot \\
& \left\{ 1 - c^2\gamma_{mn}^2 \frac{1}{30} \left(3 - 5\frac{\zeta^2}{c^2} \right) + O(c^4) \right\},
\end{aligned}$$

$$\begin{aligned}
\sigma_{23} = & \frac{a}{2h\gamma_{mn}^2} q_{mn} (n\pi\alpha) \sin m\pi\xi_1 \cos n\pi\alpha\xi_2 \left(3 - \frac{\zeta^2}{c^2} \right) \cdot \\
& \left\{ 1 - c^2\gamma_{mn}^2 \frac{1}{30} \left(3 - 5\frac{\zeta^2}{c^2} \right) + O(c^4) \right\},
\end{aligned}$$

$$\begin{aligned}
\sigma_{33} = & \frac{a}{h} q_{mn} \zeta \sin m\pi\xi_1 \sin n\pi\alpha\xi_2 \cdot \\
& \left\{ \frac{1}{6} \left(9 - \frac{\zeta^2}{c^2} \right) - c^2\gamma_{mn}^2 \frac{1}{60} \left(9 - 6\frac{\zeta^2}{c^2} + \frac{\zeta^4}{c^4} \right) + O(c^4) \right\}.
\end{aligned}$$

Note that the stresses are of different order of magnitudes. Since $\zeta \sim \frac{h}{a}$, the leading terms are

$$\begin{aligned}
\sigma_{\alpha\beta} & \sim \frac{a^2}{h^2} q_{mn}, \\
\sigma_{\alpha 3} & \sim \frac{a}{h} q_{mn}, \\
\sigma_{33} & \sim q_{mn}.
\end{aligned} \tag{3.22}$$

Thus

$$\sigma_{\alpha\beta} \gg \sigma_{\alpha 3} \gg \sigma_{33} \text{ for } \frac{h}{a} \ll 1. \tag{3.23}$$

Note further that the displacements and stresses satisfy the boundary conditions of the three-dimensional elasticity boundary-value problem (2.10) up to their respective order. Finally, the stresses satisfy the local equilibrium conditions (3.13).

4. Three-dimensional elasticity theory solutions

4.1 Solution of Saidi et al. (2009)

Based on a reformulation of Navier's equations of the three-dimensional theory of elasticity, Saidi et al. (2009) gave a closed form solution for the simply supported plate continuum. The loads applied at the faces $\zeta = \pm h/(2a)$ are developed in Fourier series and so are the displacements u_j . Since the trigonometric functions form an orthogonal function base, it is sufficient to consider only one arbitrary term. In our denotation we have

$$\begin{aligned} q &= q_{mn} \sin m\pi\xi_1 \sin n\pi\alpha\xi_2, \\ u_1 &= U_{1mn} \cos m\pi\xi_1 \sin n\pi\alpha\xi_2, \\ u_2 &= U_{2mn} \sin m\pi\xi_1 \cos n\pi\alpha\xi_2, \\ u_3 &= U_{3mn} \sin m\pi\xi_1 \sin n\pi\alpha\xi_2. \end{aligned} \quad (4.1)$$

The Fourier coefficients U_{jmn} are functions of ζ and depend on integration constants C_1, \dots, C_4 as follows

$$\begin{aligned} U_{3mn} &= C_1 \sinh \sqrt{(m\pi)^2 + (n\pi\alpha)^2} \zeta + C_2 \cosh \sqrt{(m\pi)^2 + (n\pi\alpha)^2} \zeta \\ &\quad + C_3 a \zeta \sinh \sqrt{(m\pi)^2 + (n\pi\alpha)^2} \zeta + C_4 a \zeta \cosh \sqrt{(m\pi)^2 + (n\pi\alpha)^2} \zeta, \\ U_{1mn} &= \frac{m\pi a}{(m\pi)^2 + (n\pi\alpha)^2} \left\{ \left[\frac{1}{a} \sqrt{(m\pi)^2 + (n\pi\alpha)^2} C_2 + (3-4\nu)C_3 - \right. \right. \\ &\quad \left. \left. + \sqrt{(m\pi)^2 + (n\pi\alpha)^2} \zeta C_4 \right] \sinh \sqrt{(m\pi)^2 + (n\pi\alpha)^2} \zeta \right. \\ &\quad \left. + \left[\frac{1}{a} \sqrt{(m\pi)^2 + (n\pi\alpha)^2} C_1 + (3-4\nu)C_4 \right. \right. \\ &\quad \left. \left. + \sqrt{(m\pi)^2 + (n\pi\alpha)^2} \zeta C_3 \right] \cosh \sqrt{(m\pi)^2 + (n\pi\alpha)^2} \zeta, \right. \end{aligned} \quad (4.2)$$

$$U_{2mn} = \frac{n}{m} \alpha U_{1mn}.$$

The dependence of the solution on two further constants C_5 and C_6 , which are introduced in Saidi et al (2009), have been omitted here, since they turn out to be zero for this boundary-value problem. It may be noted that in the equations (29.1) and (29.2) of Saidi et al. (2009), the minus signs before the terms $\zeta \sinh \sqrt{(m\pi)^2 + (n\pi\alpha)^2} \zeta$ and $\zeta \cosh \sqrt{(m\pi)^2 + (n\pi\alpha)^2} \zeta$ have to be replaced by plus signs (misprint). The integration constants have to be evaluated from the boundary conditions at $\zeta = \pm h/(2a)$.

In contrary to Saidi et al. (2009), we employ for σ_{33} the symmetrized boundary conditions. Thus

$$\begin{aligned}\sigma_{13}\Big|_{\zeta=\pm\frac{h}{2a}} &= \sigma_{23}\Big|_{\zeta=\pm\frac{h}{2a}} = 0, \\ \sigma_{33}\Big|_{\zeta=\pm\frac{h}{2a}} &= \pm\frac{1}{2}q\end{aligned}\tag{4.3}$$

and find with (2.5₆)

$$\begin{aligned}C_1 &= 0, \\ C_2 &= \frac{1+\nu}{E}q_{mn}a\frac{2(1-\nu)\cosh\left(\gamma_{mn}\frac{h}{2a}\right) + \frac{h}{2a}\sinh\left(\gamma_{mn}\frac{h}{2a}\right)}{\sinh\left(\gamma_{mn}\frac{h}{2a}\right) - \gamma_{mn}\frac{h}{a}}, \\ C_3 &= -\frac{1+\nu}{E}q_{mn}\frac{\cosh\left(\gamma_{mn}\frac{h}{2a}\right)}{\sinh\left(\gamma_{mn}\frac{h}{2a}\right) - \gamma_{mn}\frac{h}{a}}, \\ C_4 &= 0.\end{aligned}\tag{4.4}$$

With it, displacements and stresses can readily be evaluated as

$$\begin{aligned}u_1 &= \frac{1+\nu}{E}a\pi q_{mn}\frac{m}{\gamma_{mn}^2}\frac{\cos m\pi\xi_1 \sin n\pi\alpha\xi_2}{\sinh\left(\gamma_{mn}\frac{h}{2a}\right) - \gamma_{mn}\frac{h}{a}} \\ &\quad \left\{ -(1-2\nu)\cosh\left(\gamma_{mn}\frac{h}{2a}\right)\sinh(\gamma_{mn}\zeta) \right. \\ &\quad \left. + \gamma_{mn}\left[\frac{h}{2a}\sinh\left(\gamma_{mn}\frac{h}{2a}\right)\sinh(\gamma_{mn}\zeta) - \zeta\cosh\left(\gamma_{mn}\frac{h}{2a}\right)\cosh(\gamma_{mn}\zeta)\right] \right\},\end{aligned}\tag{4.5}$$

$$\begin{aligned}u_3 &= \frac{1+\nu}{E}aq_{mn}\frac{\sin m\pi\xi_1 \sin n\pi\alpha\xi_2}{\sinh\left(\gamma_{mn}\frac{h}{2a}\right) - \gamma_{mn}\frac{h}{a}} \\ &\quad \left\{ \frac{2(1-\nu)}{\gamma_{mn}}\cosh\left(\gamma_{mn}\frac{h}{2a}\right)\cosh(\gamma_{mn}\zeta) \right. \\ &\quad \left. + \frac{h}{2a}\sinh\left(\gamma_{mn}\frac{h}{2a}\right)\cosh(\gamma_{mn}\zeta) - \zeta\cosh\left(\gamma_{mn}\frac{h}{2a}\right)\sinh(\gamma_{mn}\zeta) \right\};\end{aligned}$$

$$\begin{aligned}
\sigma_{11} &= \frac{q_{mn}}{\gamma_{mn}^2} \frac{\sin m\pi\xi_1 \sin n\pi\alpha\xi_2}{\sinh\left(\gamma_{mn}\frac{h}{a}\right) - \gamma_{mn}\frac{h}{a}} \cdot \\
&\quad \left\{ \cosh\left(\gamma_{mn}\frac{h}{2a}\right) \sinh(\gamma_{mn}\zeta) \left((m\pi)^2 + 2\nu(n\pi\alpha)^2 \right) \right. \\
&\quad \left. + \gamma_{mn}(m\pi)^2 \left[-\frac{h}{2a} \sinh\left(\gamma_{mn}\frac{h}{2a}\right) \sinh(\gamma_{mn}\zeta) + \zeta \cosh\left(\gamma_{mn}\frac{h}{2a}\right) \cosh(\gamma_{mn}\zeta) \right] \right\}, \\
\sigma_{12} &= \frac{\pi^2 mn\alpha q_{mn}}{\gamma_{mn}^2} \frac{\cos m\pi\xi_1 \cos n\pi\alpha\xi_2}{\sinh\left(\gamma_{mn}\frac{h}{a}\right) - \gamma_{mn}\frac{h}{a}} \cdot \\
&\quad \left\{ -(1-2\nu) \cosh\left(\gamma_{mn}\frac{h}{2a}\right) \sinh(\gamma_{mn}\zeta) \right. \\
&\quad \left. + \gamma_{mn} \left[\frac{h}{2a} \sinh\left(\gamma_{mn}\frac{h}{2a}\right) \sinh(\gamma_{mn}\zeta) - \zeta \cosh\left(\gamma_{mn}\frac{h}{2a}\right) \cosh(\gamma_{mn}\zeta) \right] \right\}
\end{aligned} \tag{4.6}$$

$$\begin{aligned}
\sigma_{13} &= \frac{1}{2} m\pi q_{mn} \frac{\cos m\pi\xi_1 \sin n\pi\alpha\xi_2}{\sinh\left(\gamma_{mn}\frac{h}{a}\right) - \gamma_{mn}\frac{h}{a}} \cdot \\
&\quad \left\{ \frac{h}{a} \sinh\left(\gamma_{mn}\frac{h}{2a}\right) \cosh(\gamma_{mn}\zeta) - 2\zeta \cosh\left(\gamma_{mn}\frac{h}{2a}\right) \sinh(\gamma_{mn}\zeta) \right\}
\end{aligned}$$

$$\begin{aligned}
\sigma_{33} &= q_{mn} \frac{\sin m\pi\xi_1 \sin n\pi\alpha\xi_2}{\sinh\left(\gamma_{mn}\frac{h}{a}\right) - \gamma_{mn}\frac{h}{a}} \cdot \left\{ \cosh\left(\gamma_{mn}\frac{h}{2a}\right) \sinh(\gamma_{mn}\zeta) \right. \\
&\quad \left. + \gamma_{mn} \left[\frac{h}{2a} \sinh\left(\gamma_{mn}\frac{h}{2a}\right) \sinh(\gamma_{mn}\zeta) - \zeta \cosh\left(\gamma_{mn}\frac{h}{2a}\right) \cosh(\gamma_{mn}\zeta) \right] \right\}.
\end{aligned}$$

The displacement u_2 follows from u_1 by replacing $m \cos m\pi\xi_1 \sin n\pi\alpha\xi_2$ in the first row of (4.5₁) by $n\alpha \sin m\pi\xi_1 \cos n\pi\alpha$. The stress σ_{22} follows from σ_{11} by replacing $(m\pi)^2 + 2\nu(n\pi\alpha)^2$ by $(n\pi\alpha)^2 + 2\nu(m\pi)^2$ in the second and $(m\pi)^2$ by $(n\pi\alpha)^2$ in the third line of (4.6₁). The stress σ_{23} is obtained by replacing $m\pi q_{mn} \cos m\pi\xi_1 \sin n\pi\alpha\xi_2$ by $n\pi\alpha q_{mn} \sin m\pi\xi_1 \cos n\pi\alpha\xi_2$ in the first line of (4.6₃). It is seen immediately that

$\sigma_{13}|_{\zeta=\pm\frac{h}{2a}} = \sigma_{23}|_{\zeta=\pm\frac{h}{2a}} = 0$ and $\sigma_{33}|_{\zeta=\pm\frac{h}{2a}} = \pm\frac{1}{2}q$, i.e., the boundary conditions along the plate faces are satisfied. The boundary conditions (2.10) along $\xi_1 = 0,1$ and $\alpha\xi_2 = 0,1$ are satisfied likewise.

4.2 Solution using displacement potentials of Youngdahl (1969)

Following Youngdahl (1969), the displacements in a homogeneous isotropic solid can be represented in terms of three harmonic functions ϕ_1, ϕ_2, ϕ_3 in the form

$$\begin{aligned} u_1 &= \frac{\partial \phi_1}{\partial x_1} - \frac{x_3}{4(1-\nu)} \frac{\partial^2 \phi_2}{\partial x_1 \partial x_3} + \frac{\partial \phi_3}{\partial x_2}, \\ u_2 &= \frac{\partial \phi_1}{\partial x_2} - \frac{x_3}{4(1-\nu)} \frac{\partial^2 \phi_2}{\partial x_2 \partial x_3} - \frac{\partial \phi_3}{\partial x_1}, \\ u_3 &= \frac{\partial \phi_1}{\partial x_3} - \frac{x_3}{4(1-\nu)} \frac{\partial^2 \phi_2}{\partial x_3^2} + \frac{3-4\nu}{4(1-\nu)} \frac{\partial \phi_2}{\partial x_3} \end{aligned} \quad (4.7)$$

Substituting the above representation (4.7) into the stress-displacement relations, the representation for stresses can be derived as

$$\begin{aligned} \sigma_{11} &= G \left[2 \frac{\partial^2 \phi_1}{\partial x_1^2} - \frac{x_3}{2(1-\nu)} \frac{\partial^3 \phi_2}{\partial x_1^2 \partial x_3} + \frac{\nu}{(1-\nu)} \frac{\partial^2 \phi_2}{\partial x_3^2} + 2 \frac{\partial^2 \phi_3}{\partial x_1 \partial x_2} \right], \\ \sigma_{22} &= G \left[2 \frac{\partial^2 \phi_1}{\partial x_2^2} - \frac{x_3}{2(1-\nu)} \frac{\partial^3 \phi_2}{\partial x_2^2 \partial x_3} + \frac{\nu}{(1-\nu)} \frac{\partial^2 \phi_2}{\partial x_3^2} - 2 \frac{\partial^2 \phi_3}{\partial x_1 \partial x_2} \right], \\ \sigma_{33} &= G \left[2 \frac{\partial^2 \phi_1}{\partial x_3^2} - \frac{x_3}{2(1-\nu)} \frac{\partial^3 \phi_2}{\partial x_3^3} + \frac{\partial^2 \phi_2}{\partial x_3^2} \right], \end{aligned} \quad (4.8)$$

$$\begin{aligned} \sigma_{23} &= G \left[2 \frac{\partial^2 \phi_1}{\partial x_2 \partial x_3} - \frac{x_3}{2(1-\nu)} \frac{\partial^3 \phi_2}{\partial x_2 \partial x_3^2} + \frac{1-2\nu}{2(1-\nu)} \frac{\partial^2 \phi_2}{\partial x_2 \partial x_3} - \frac{\partial^2 \phi_3}{\partial x_1 \partial x_3} \right], \\ \sigma_{13} &= G \left[2 \frac{\partial^2 \phi_1}{\partial x_1 \partial x_3} - \frac{x_3}{2(1-\nu)} \frac{\partial^3 \phi_2}{\partial x_1 \partial x_3^2} + \frac{1-2\nu}{2(1-\nu)} \frac{\partial^2 \phi_2}{\partial x_1 \partial x_3} + \frac{\partial^2 \phi_3}{\partial x_2 \partial x_3} \right], \\ \sigma_{12} &= G \left[2 \frac{\partial^2 \phi_1}{\partial x_1 \partial x_2} - \frac{x_3}{2(1-\nu)} \frac{\partial^3 \phi_2}{\partial x_1 \partial x_2 \partial x_3} + \left(\frac{\partial^2 \phi_3}{\partial x_2^2} - \frac{\partial^2 \phi_3}{\partial x_1^2} \right) \right] \end{aligned}$$

(shear modulus $G = E/(2(1+\nu))$).

Guided by the loading distribution (2.3) and boundary conditions (2.10), the three harmonic functions can be chosen in the form

$$\begin{aligned} \phi_1 &= (A_1 \cosh \lambda x_3 + A_2 \sinh \lambda x_3) \sin \frac{\pi m x_1}{a} \sin \frac{\pi n x_2}{b}, \\ \phi_2 &= (A_3 \cosh \lambda x_3 + A_4 \sinh \lambda x_3) \sin \frac{\pi m x_1}{a} \sin \frac{\pi n x_2}{b}, \\ \phi_3 &= (A_5 \cosh \lambda x_3 + A_6 \sinh \lambda x_3) \cos \frac{\pi m x_1}{a} \cos \frac{\pi n x_2}{b}, \end{aligned} \quad (4.9)$$

$$\lambda = \sqrt{\left[\left(\frac{\pi m}{a}\right)^2 + \left(\frac{\pi n}{b}\right)^2\right]}.$$

The form (4.9) allows for the boundary conditions (2.10) at the edges of the plate to be satisfied identically. The six unknown constants A_k ($k=1, \dots, 6$) can be determined from the boundary conditions (2.4) at the top and bottom faces of the plate. In the problem formulated in Section 2, they are found to be

$$A_1 = 0, \quad A_2 = \frac{q_{mn}}{G} \frac{\alpha_2}{\beta}, \quad A_3 = 0, \quad A_4 = \frac{q_{mn}}{G} \frac{1}{\beta}, \quad A_5 = 0, \quad A_6 = 0 \quad (4.10)$$

where

$$\alpha_2 = \frac{1}{4 \cosh\left(\lambda \frac{h}{2}\right)} \left[\frac{\lambda h}{2(1-\nu)} \sinh\left(\lambda \frac{h}{2}\right) - \frac{1-2\nu}{1-\nu} \cosh\left(\lambda \frac{h}{2}\right) \right] \quad (4.11)$$

$$\beta = 2\lambda^2(2\alpha_2 + 1) \sinh\left(\lambda \frac{h}{2}\right) - \frac{\lambda h}{2(1-\nu)} \lambda^2 \cosh\left(\lambda \frac{h}{2}\right),$$

Then the closed-form expressions for stresses and displacements are obtained as

$$u_1 = \frac{q_{mn}}{G} \frac{1}{\beta} \left(\frac{\pi m}{a}\right) \left[\alpha_2 \sinh \lambda x_3 - \frac{\lambda x_3}{4(1-\nu)} \cosh \lambda x_3 \right] \cos \frac{\pi m x_1}{a} \sin \frac{\pi n x_2}{b},$$

$$u_2 = \frac{q_{mn}}{G} \frac{1}{\beta} \left(\frac{\pi n}{b}\right) \left[\alpha_2 \sinh \lambda x_3 - \frac{\lambda x_3}{4(1-\nu)} \cosh \lambda x_3 \right] \sin \frac{\pi m x_1}{a} \cos \frac{\pi n x_2}{b}, \quad (4.12)$$

$$u_3 = \frac{q_{mn}}{G} \frac{\lambda}{\beta} \left[\left(\alpha_2 + \frac{3-4\nu}{4(1-\nu)} \right) \cosh \lambda x_3 - \frac{\lambda x_3}{4(1-\nu)} \sinh \lambda x_3 \right] \sin \frac{\pi m x_1}{a} \sin \frac{\pi n x_2}{b}.$$

$$\sigma_{33} = \frac{q_{mn}}{\beta} \lambda^2 \sin \frac{\pi m x_1}{a} \sin \frac{\pi n x_2}{b} \times$$

$$\times \left[(2\alpha_2 + 1) \sinh \lambda x_3 - \frac{\lambda x_3}{2(1-\nu)} \cosh \lambda x_3 \right]$$

$$\sigma_{13} = \frac{q_{mn}}{\beta} \lambda \left(\frac{\pi m}{a}\right) \cos \frac{\pi m x_1}{a} \sin \frac{\pi n x_2}{b} \times$$

$$\times \left[\left(2\alpha_2 + \frac{1-2\nu}{2(1-\nu)} \right) \cosh \lambda x_3 - \frac{\lambda x_3}{2(1-\nu)} \sinh \lambda x_3 \right]$$

$$\begin{aligned} \sigma_{23} &= \frac{q_{mn}}{\beta} \lambda \left(\frac{\pi n}{b} \right) \sin \frac{\pi m x_1}{a} \cos \frac{\pi n x_2}{b} \times \\ &\times \left[\left(2\alpha_2 + \frac{1-2\nu}{2(1-\nu)} \right) \cosh \lambda x_3 - \frac{\lambda x_3}{2(1-\nu)} \sinh \lambda x_3 \right] \end{aligned} \quad (4.13)$$

$$\begin{aligned} \sigma_{11} &= \frac{q_{mn}}{\beta} \sin \frac{\pi m x_1}{a} \sin \frac{\pi n x_2}{b} \times \\ &\times \left[\left(-2\alpha_2 \left(\frac{\pi m}{a} \right)^2 + \lambda^2 \frac{\nu}{1-\nu} \right) \sinh \lambda x_3 + \frac{\lambda x_3}{2(1-\nu)} \left(\frac{\pi m}{a} \right)^2 \cosh \lambda x_3 \right] \end{aligned}$$

$$\begin{aligned} \sigma_{22} &= \frac{q_{mn}}{\beta} \sin \frac{\pi m x_1}{a} \sin \frac{\pi n x_2}{b} \times \\ &\times \left[\left(-2\alpha_2 \left(\frac{\pi n}{b} \right)^2 + \lambda^2 \frac{\nu}{1-\nu} \right) \sinh \lambda x_3 + \frac{\lambda x_3}{2(1-\nu)} \left(\frac{\pi n}{b} \right)^2 \cosh \lambda x_3 \right] \end{aligned}$$

$$\begin{aligned} \sigma_{12} &= \frac{q_{mn}}{\beta} \cos \frac{\pi m x_1}{a} \cos \frac{\pi n x_2}{b} \times \\ &\times \left(\frac{\pi m}{a} \right) \left(\frac{\pi n}{b} \right) \left[2\alpha_2 \sinh \lambda x_3 - \frac{\lambda x_3}{2(1-\nu)} \cosh \lambda x_3 \right] \end{aligned}$$

As the solution of the boundary-value problem in three-dimensional elasticity is unique, the above closed-form expressions (4.12) – (4.13) obtained using the displacement potential method should coincide with the closed-form expressions (4.5) – (4.6) presented in Section 4.1. After substituting the quantities (4.11) into (4.12) – (4.13) and employing the notations (2.5), the closed-form expression (4.12₁) for the in-plane displacement u_1 transforms into

$$\begin{aligned} u_1 &= \frac{(1+\nu)}{E} a \pi q_{mn} \left(\frac{m}{\gamma_{mn}^2} \right) \frac{\cos m \pi \xi_1 \sin n \pi \alpha \xi_2}{\sinh \left(\gamma_{mn} \frac{h}{a} \right) - \gamma_{mn} \frac{h}{a}} \left\{ -(1-2\nu) \cosh \left(\gamma_{mn} \frac{h}{2a} \right) \sinh (\gamma_{mn} \zeta) + \right. \\ &\left. + \gamma_{mn} \left[\frac{h}{2a} \sinh \left(\gamma_{mn} \frac{h}{2a} \right) \sinh (\gamma_{mn} \zeta) - \zeta \cosh \left(\gamma_{mn} \frac{h}{2a} \right) \cosh (\gamma_{mn} \zeta) \right] \right\} \end{aligned} \quad (4.14)$$

The above expression coincides with (4.5₁) given in Section 4.1.

Similarly, the closed-form expression (4.12₃) for the transverse displacement u_3 transforms into

$$\begin{aligned}
u_3 = & \frac{(1+\nu)}{E} a q_{mn} \frac{\sin \pi m \xi_1 \sin \pi n \alpha \xi_2}{\sinh\left(\gamma_{mn} \frac{h}{a}\right) - \gamma_{mn} \frac{h}{a}} \left\{ \frac{2(1-\nu)}{\gamma_{mn}} \cosh\left(\gamma_{mn} \frac{h}{2a}\right) \cosh(\gamma_{mn} \zeta) + \right. \\
& \left. + \frac{h}{2a} \sinh\left(\gamma_{mn} \frac{h}{2a}\right) \cosh(\gamma_{mn} \zeta) - \zeta \cosh\left(\gamma_{mn} \frac{h}{2a}\right) \sinh(\gamma_{mn} \zeta) \right\}
\end{aligned} \tag{4.15}$$

The above expression coincides with (4.5₂) given in Section 4.1. Thus, it is evident that the closed-form expressions (4.12) – (4.13) for displacements and stresses obtained using Youngdahl's displacement potentials satisfy the uniqueness of solution requirement.

5. Taylor series expansion and comparisons

It has been proved in Schneider et al. (2014) that consistent higher-order plate theories are Taylor-series expansions of N-th order of the exact solution of the three-dimensional theory of elasticity. It is thus intriguing to develop the exact three-dimensional elasticity solution into a power series in h/a and show the equivalence of the first terms. It is sufficient to show the correspondence for the displacements u_j . Due to Hooke's law the correspondence for the stresses in turn is obvious.

When using formulae for the Taylor-series expansions, we frequently take recourse to Bronstein & Semendjajev (1996). We start with

$$\begin{aligned}
\sinh\left(\gamma_{mn} \frac{h}{a}\right) - \gamma_{mn} \frac{h}{a} = & \frac{1}{6} \gamma_{mn}^3 \frac{h^3}{a^3} \left(1 + \frac{1}{20} \left(\gamma_{mn} \frac{h}{a}\right)^2 + \frac{1}{840} \left(\gamma_{mn} \frac{h}{a}\right)^4 \right. \\
& \left. + \frac{1}{60,480} \left(\gamma_{mn} \frac{h}{a}\right)^6 + O\left(\frac{h}{a}\right)^8 \right),
\end{aligned} \tag{5.1}$$

$$\begin{aligned}
\frac{1}{\sinh\left(\gamma_{mn} \frac{h}{a}\right) - \gamma_{mn} \frac{h}{a}} = & \frac{6a^3}{\gamma_{mn} h^3} \left(1 - \frac{1}{20} \left(\gamma_{mn} \frac{h}{a}\right)^2 + \frac{11}{8,400} \left(\gamma_{mn} \frac{h}{a}\right)^4 \right. \\
& \left. - \frac{17}{756,000} \left(\gamma_{mn} \frac{h}{a}\right)^6 + O\left(\frac{h}{a}\right)^8 \right).
\end{aligned}$$

For the products of the hyperbolic functions, we find

$$\begin{aligned}
\cosh \left(\gamma_{mn} \frac{h}{2a} \right) \cosh (\gamma_{mn} \zeta) &= 1 + \gamma_{mn}^2 \frac{1}{2} (3c^2 + \zeta^2) \\
&+ \gamma_{mn}^4 \frac{1}{24} (9c^4 + 18c^2 \zeta^2 + \zeta^4) \\
&+ \gamma_{mn}^6 \frac{1}{720} (27c^6 + 135c^4 \zeta^2 + 45c^2 \zeta^4 + \zeta^6) + O(c^8), \\
\sinh \left(\gamma_{mn} \frac{h}{2a} \right) \cosh (\gamma_{mn} \zeta) &= \gamma_{mn} \frac{h}{2a} \left(1 + \gamma_{mn}^2 \frac{1}{2} (c^2 + \zeta^2) \right. \\
&+ \gamma_{mn}^4 \frac{1}{120} (9c^4 + 30c^2 \zeta^2 + 5\zeta^4) \\
&\left. + \gamma_{mn}^6 \frac{1}{5,040} (27c^6 + 189c^4 \zeta^2 + 105c^2 \zeta^4 + 7\zeta^6) + O(c^8) \right), \tag{5.2}
\end{aligned}$$

$$\begin{aligned}
\cosh \left(\gamma_{mn} \frac{h}{2a} \right) \sinh (\gamma_{mn} \zeta) &= \gamma_{mn} \zeta \left(1 + \gamma_{mn}^2 \frac{1}{6} (9c^2 + \zeta^2) \right. \\
&+ \gamma_{mn}^4 \frac{1}{120} (45c^4 + 30c^2 \zeta^2 + \zeta^4) \\
&\left. + \gamma_{mn}^6 \frac{1}{5,040} (189c^6 + 315c^4 \zeta^2 + 63c^2 \zeta^4 + \zeta^6) + O(c^8) \right),
\end{aligned}$$

$$\sinh \left(\gamma_{mn} \frac{h}{2a} \right) \sinh (\gamma_{mn} \zeta) = \gamma_{mn}^2 \zeta \left(1 + \gamma_{mn}^2 \frac{1}{6} (3c^2 + \zeta^2) + O(c^4) \right).$$

Inserting (5.1) and (5.2) into (4.5) yields

$$\begin{aligned}
u_1 &= \frac{a^4 q_{mn}}{\gamma_{mn}^4 K} (m\pi) \zeta \cos m\pi \xi_1 \sin n\pi \alpha \xi_2 \cdot \\
&\left\{ -1 + c^2 \gamma_{mn}^2 \frac{1}{30} \left(9 \frac{2+3v}{1-v} - 5 \frac{2-v}{1-v} \frac{\zeta^2}{c^2} \right) \right. \\
&\left. + c^4 \gamma_{mn}^4 \left[\frac{3}{1,400} \frac{87-157v}{1-v} - \frac{1}{20} \frac{1-3v}{1-v} \frac{\zeta^2}{c^2} - \frac{1}{120} \frac{3-v}{1-v} \frac{\zeta^4}{c^4} \right] + O(c^6) \right\},
\end{aligned}$$

$$\begin{aligned}
u_3 = & \frac{a^4 q_{mn}}{\gamma_{mn}^4 K} \sin m\pi\xi_1 \sin n\pi\alpha\xi_2 \cdot \\
& \left\{ 1 + \frac{c^2 \gamma_{mn}^2}{1-\nu} \frac{1}{10} \left[3(8-3\nu) - 5\nu \frac{\zeta^2}{c^2} \right] \right. \\
& + \frac{c^4 \gamma_{mn}^4}{1-\nu} \left[-\frac{3}{1,400} (227-157\nu) + \frac{3}{20} (5-3\nu) \frac{\zeta^2}{c^2} - \frac{1}{24} (1+\nu) \frac{\zeta^4}{c^4} \right] \\
& + \frac{c^6 \gamma_{mn}^6}{1-\nu} \left[\frac{1}{14,000} (26-791\nu) - \frac{3}{2,800} (70-157\nu) \frac{\zeta^2}{c^2} \right. \\
& \left. \left. + \frac{1}{80} (2-3\nu) \frac{\zeta^4}{c^4} - \frac{1}{720} (2+\nu) \frac{\zeta^6}{c^6} \right] + O(c^8) \right\}. \tag{5.3}
\end{aligned}$$

Again, u_2 follows from u_1 by replacing $m\pi \cos m\pi\xi_1 \sin n\pi\alpha\xi_2$ in (5.3₁) by $n\pi\alpha \sin m\pi\xi_1 \cos n\pi\alpha\xi_2$.

Now, we can compare the displacements calculated from (5.3) and (3.20). First, it may be concluded that all terms not involving the constants A_1 and A_2 are in complete agreement. Comparing coefficients of the terms involving the constants A_1 and A_2 leads to the following overdetermined system of algebraic equations

$$\begin{aligned}
u_1 c^4 : & \quad -A_1 - \frac{3}{30} \frac{5+7\nu-6\nu^2}{(1-\nu)^2} = \frac{3}{1,400} \frac{87-157\nu}{1-\nu}, \\
u_3 c^4 : & \quad A_1 + \frac{9}{25} \frac{\nu(2-\nu)}{(1-\nu)^2} = -\frac{3}{1,400} \frac{227-157\nu}{1-\nu}, \\
u_3 c^4 \zeta^2 : & \quad -\frac{1}{2} \frac{\nu}{1-\nu} A_1 - \frac{3}{200} \frac{5-5\nu+24\nu^2-12\nu^3}{(1-\nu)^3} = -\frac{3}{2,800} \frac{70-157\nu}{1-\nu}, \\
u_3 c^6 : & \quad -A_2 + \frac{6}{5} \frac{2-\nu}{1-\nu} A_1 = \frac{1}{14,000} \frac{26-791\nu}{1-\nu}. \tag{5.4}
\end{aligned}$$

By choosing

$$A_1 = -\frac{3}{1,400} \frac{227-48\nu-11\nu^2}{(1-\nu)^2}, \tag{5.5}$$

the first three equations of (5.4) are identically satisfied, and A_2 follows from the fourth equation as

$$A_2 = -\frac{1}{14,000} \frac{16,370-12,471\nu+2,544\nu^2-395\nu^3}{(1-\nu)^3}, \tag{5.6}$$

a formula that would have hardly been guessed a priori.

With A_1 known, we can evaluate the stresses $\sigma_{\alpha\beta}$ up to the order $O(c^6)$ from (3.8₁₋₃) as

$$\begin{aligned} \sigma_{11} = & \frac{a\zeta}{hc^2} \frac{q_{mn}}{\gamma_{mn}^4} \sin m\pi\xi_1 \sin n\pi\alpha\xi_2 \cdot \\ & \left\{ (m\pi)^2 + \nu(n\pi\alpha)^2 + c^2\gamma_{mn}^2 \frac{1}{30} \left[-18(m\pi)^2 + 27\nu(n\pi\alpha)^2 + (10(m\pi)^2 + 5\nu(n\pi\alpha)^2) \frac{\zeta^2}{c^2} \right] \right. \\ & + c^4\gamma_{mn}^4 \left[-\frac{3}{1,400} (87(m\pi)^2 + 157\nu(n\pi\alpha)^2) \right. \\ & \left. \left. + \frac{1}{20} ((m\pi)^2 + 3\nu(n\pi\alpha)^2) \frac{\zeta^2}{c^2} + \frac{1}{120} (3(m\pi)^2 + \nu(n\pi\alpha)^2) \frac{\zeta^4}{c^4} \right] + O(c^6) \right\} \end{aligned} \quad (5.7)$$

$$\begin{aligned} \sigma_{22} = & \frac{a\zeta}{hc^2} \frac{q_{mn}}{\gamma_{mn}^4} \sin m\pi\xi_1 \sin n\pi\alpha\xi_2 \cdot \\ & \left\{ (n\pi\alpha)^2 + \nu(m\pi)^2 + c^2\gamma_{mn}^2 \frac{1}{30} \left[-18(n\pi\alpha)^2 + 27\nu(m\pi)^2 + (10(n\pi\alpha)^2 + 5\nu(m\pi)^2) \frac{\zeta^2}{c^2} \right] \right. \\ & + c^4\gamma_{mn}^4 \left[-\frac{3}{1,400} (87(n\pi\alpha)^2 + 157\nu(m\pi)^2) \right. \\ & \left. \left. + \frac{1}{20} ((n\pi\alpha)^2 + 3\nu(m\pi)^2) \frac{\zeta^2}{c^2} + \frac{1}{120} (3(n\pi\alpha)^2 + \nu(m\pi)^2) \frac{\zeta^4}{c^4} \right] + O(c^6) \right\} \end{aligned}$$

$$\begin{aligned} \sigma_{12} = & \frac{a\zeta}{hc^2} \frac{q_{mn}}{\gamma_{mn}^4} (m\pi)(n\pi\alpha) \cos m\pi\xi_1 \cos n\pi\alpha\xi_2 \cdot \\ & \left\{ -(1-\nu) + c^2\gamma_{mn}^2 \frac{1}{30} \left[9(2+3\nu) - 5(2-\nu) \frac{\zeta^2}{c^2} \right] \right. \\ & \left. + c^4\gamma_{mn}^4 \left[\frac{3}{1,400} (87-157\nu) - \frac{1}{20} (1-3\nu) \frac{\zeta^2}{c^2} - \frac{1}{120} (3-\nu) \frac{\zeta^4}{c^4} \right] + O(c^6) \right\}. \end{aligned}$$

In conclusion it may be stated that the displacements and stresses calculated from the consistent second-order plate theory (denoted with the superscript (P)) coincide with those of the three-dimensional elasticity theory (denoted with the superscript (E)) modulo higher order terms as

$$\begin{aligned}
u_\alpha^{(E)} &= u_\alpha^{(P)} + O(c^7), \\
u_3^{(E)} &= u_3^{(P)} + O(c^8), \\
\sigma_{\alpha\beta}^{(E)} &= \sigma_{\alpha\beta}^{(P)} + O(c^7), \\
\sigma_{\alpha 3}^{(E)} &= \sigma_{\alpha 3}^{(P)} + O(c^4), \\
\sigma_{33}^{(E)} &= \sigma_{33}^{(P)} + O(c^5).
\end{aligned} \tag{5.8}$$

6. Parametric study

In this section, a parametric study for the special case of $m = n = \alpha = 1$ is performed, i.e. we take the formulae for the quadratic plate $a = b$ under a single-wave external load from the previous sections and replace q_{11} with P_0 . In order to simplify the parametric evaluation we introduce a new thickness variable $\bar{\zeta}$ as

$$\bar{\zeta} = \frac{x_3}{h} \Rightarrow \zeta = \frac{h}{a} \bar{\zeta}, \quad \frac{\zeta^2}{c^2} = 12\bar{\zeta}^2, \quad -\frac{1}{2} \leq \bar{\zeta} \leq +\frac{1}{2} \tag{6.1}$$

The formulae are interpreted as $f = f(\xi_1, \xi_2, \bar{\zeta})$. We compare maximum values of the second-order consistent plate theory (P) and the three-dimensional elasticity theory (E) for the displacements and stresses by introducing non-dimensional quantities. Wherever numerical values are presented, we choose $\nu = 0.3$ for Poisson's ratio. A comparison with other consistent second-order theories like, e. g., the Reissner-Mindlin theory, is not necessary, since it has been shown in Kienzler and Schneider (2017) that they are equivalent within the second-order approximation.

We start with the in-plane displacement and introduce

$$\bar{u}_1(\bar{\zeta}) = -\frac{8\pi^3 K}{a^3 h P_0} u_1\left(0, \frac{1}{2}, \bar{\zeta}\right) = -\frac{8\pi^3 K}{a_3 h P_0} u_2\left(\frac{1}{2}, 0, \bar{\zeta}\right). \tag{6.2}$$

For (P) we have from (5.3₁)

$$\begin{aligned}
\bar{u}_1^{(P)}(\bar{\zeta}) &= 2\bar{\zeta} \left\{ 1 - \frac{h^2 \pi^2}{a^2} \left(\frac{1}{20} \frac{2+3\nu}{1-\nu} - \frac{1}{3} \frac{2-\nu}{1-\nu} \bar{\zeta}^2 \right) \right. \\
&\quad \left. - \frac{h^4 \pi^4}{a^4} \left(\frac{1}{16,800} \frac{87-157\nu}{1-\nu} - \frac{1}{60} \frac{1-3\nu}{1-\nu} \bar{\zeta}^2 - \frac{1}{30} \frac{3-\nu}{1-\nu} \bar{\zeta}^4 \right) + O\left(\frac{h^6}{a^6}\right) \right\}.
\end{aligned} \tag{6.3}$$

For (E) we find with (4.5₁)

$$\begin{aligned} \bar{u}_1^{(E)}(\bar{\zeta}) &= \frac{h^2 \pi^2}{3a^2(1-\nu)} \cdot \frac{1}{\sinh\left(\sqrt{2} \frac{h\pi}{a}\right) - \sqrt{2} \frac{h\pi}{a}} \\ &\quad \left\{ (1-2\nu) \cosh\left(\sqrt{2} \frac{h\pi}{2a}\right) \sinh\left(\sqrt{2} \frac{h\pi}{a} \bar{\zeta}\right) \right. \\ &\quad \left. + \frac{1}{2} \sqrt{2} \frac{h\pi}{a} \left(2\bar{\zeta} \cosh\left(\sqrt{2} \frac{h\pi}{2a}\right) \cosh\left(\sqrt{2} \frac{h\pi}{a} \bar{\zeta}\right) \right) \right. \\ &\quad \left. - \sinh\left(\sqrt{2} \frac{h\pi}{2a}\right) \sinh\left(\sqrt{2} \frac{h\pi}{a} \bar{\zeta}\right) \right\} \end{aligned} \quad (6.4)$$

with

$$\lim_{\frac{h}{a} \rightarrow 0} \bar{u}_1^{(E)}(\bar{\zeta}) = 2\bar{\zeta}. \quad (6.5)$$

Especially for $\bar{\zeta} = \frac{1}{2}$, we find

$$\begin{aligned} \bar{u}_1^{(P)}(1/2) &= 1 + \frac{h^2 \pi^2}{a^2} \frac{1}{30} \frac{2-7\nu}{1-\nu} + \frac{h^4 \pi^4}{a^4} \frac{11}{2.100} \\ &= 1 - 0.046998 \frac{h^2}{a^2} + 0.510238 \frac{h^4}{a^4} \end{aligned} \quad (6.6)$$

$$\bar{u}_1^{(E)}(1/2) = \frac{h^2 \pi^2}{6a^2(1-\nu)} \frac{(1-2\nu) \sinh\left(\sqrt{2} \frac{h\pi}{a}\right) + \sqrt{2} \frac{h\pi}{a}}{\sinh\left(\sqrt{2} \frac{h\pi}{a}\right) - \sqrt{2} \frac{h\pi}{a}}. \quad (6.7)$$

A comparison of both values for different ratios h/a is given in Table 1, where we restricted ourselves to four digit after the comma for perspicuity.

Table 1. Values for the displacement \bar{u}_1

| $\frac{h}{a}$ | 0 | $\frac{1}{10}$ | $\frac{1}{5}$ | $\frac{1}{3}$ | $\frac{1}{2}$ |
|----------------------|---|----------------|---------------|---------------|---------------|
| $\bar{u}^{(P)}(1/2)$ | 1 | 0.9996 | 0.9989 | 1.0011 | 1.0201 |
| $\bar{u}^{(E)}(1/2)$ | 1 | 0.9996 | 0.9989 | 1.0009 | 1.0176 |
| $\Delta \%$ | 0 | 0.00 | 0.00 | 0.02 | 0.25 |

Fig. 6 shows the distribution of $\bar{u}_1^{(E)} = \left(\bar{\zeta}, \frac{h}{a} \right)$ along the thickness of the plate for various values of the parameter h/a . A significant deviation from the plane cross-section starts with $h/a > 1/5$ and is quite pronounced for $h/a = 1/2$. The deviation between the plate solution $\bar{u}_1^{(P)} = \left(\bar{\zeta}, \frac{h}{a} \right)$ and the exact elasticity solution $\bar{u}_1^{(E)} = \left(\bar{\zeta}, \frac{h}{a} \right)$ remains far less than 1% even for values $h/a = 1/2$. In the example shown in Fig. 7, the difference between both solutions is practically not to be seen, The maximal deviation occurs at $\bar{\zeta} = \pm 1/2$ coinciding with the values given in Table 1.

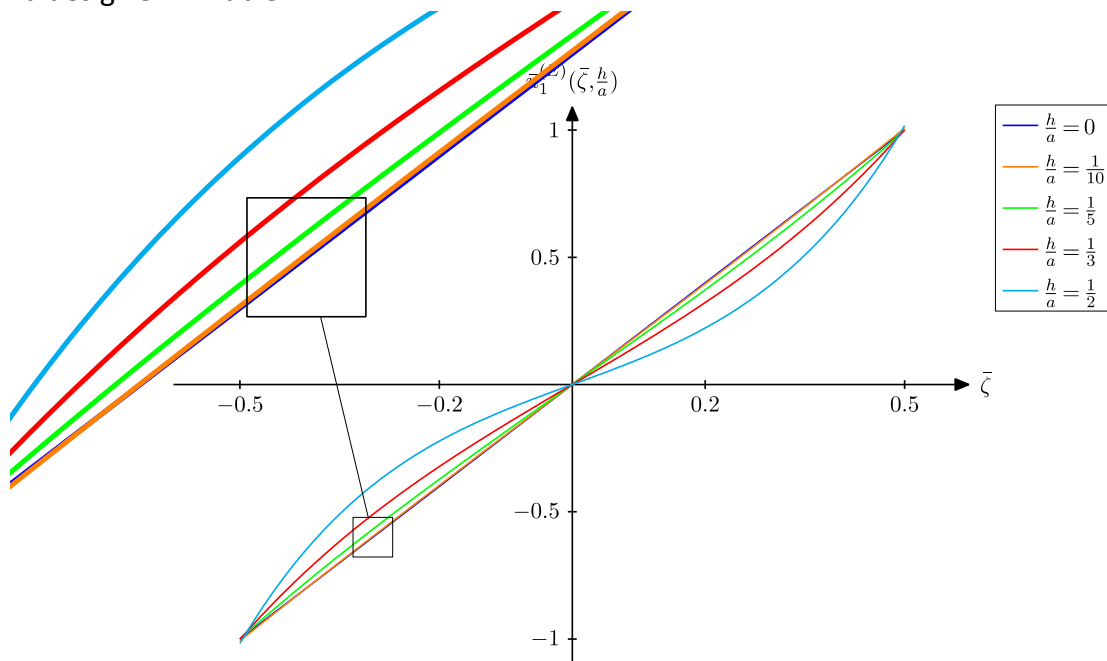


Fig. 6. In plane displacement $\bar{u}_1^{(E)} = \left(\bar{\zeta}, \frac{h}{a} \right)$ along the plate thickness with h/a as parameter

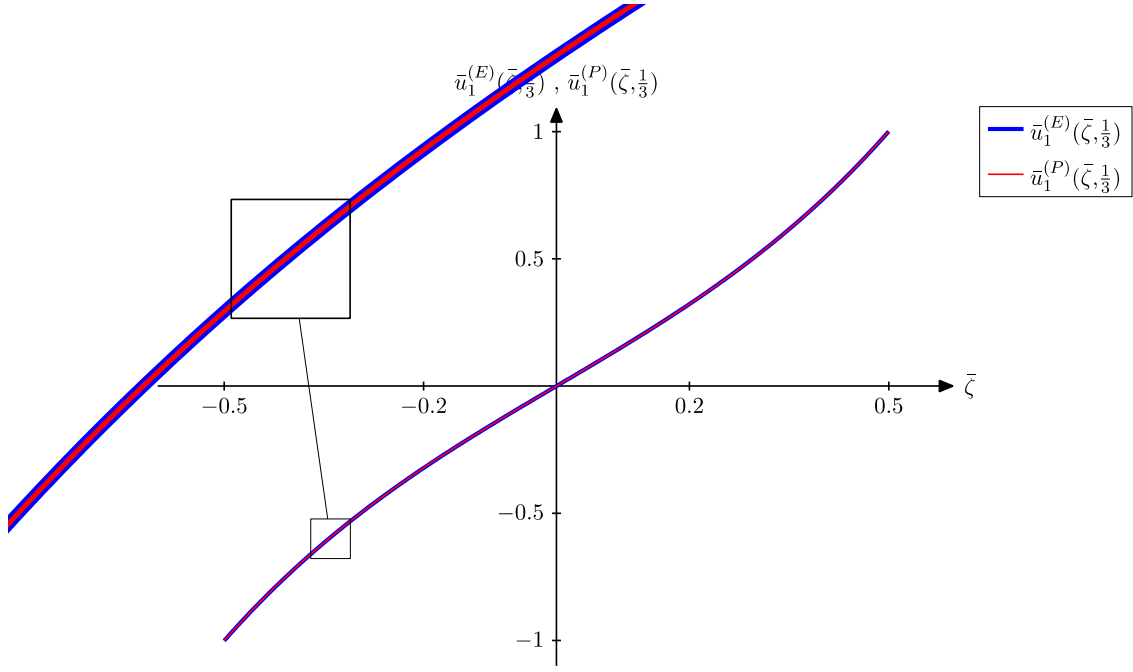


Fig. 7. Comparison between the exact elasticity solution $\bar{u}_1^{(E)}$ and $\bar{u}_1^{(P)}$ along the non-dimensionalised thickness coordinate $\bar{\zeta}$ for $h/a = 1/3$

For the displacement in x_3 -direction, we introduce

$$\bar{u}_3(\bar{\zeta}) = \frac{4\pi^4 K}{a^4 P_0} u_3\left(\frac{1}{2}, \frac{1}{2}, \bar{\zeta}\right) \quad (6.8)$$

and find from (5.3₂)

$$\begin{aligned} \bar{u}_3^{(P)}(\bar{\zeta}) = & 1 + \frac{h^2 \pi^2}{a^2} \left(\frac{1}{20} \frac{8-3\nu}{1-\nu} - \frac{\nu}{1-\nu} \bar{\zeta}^2 \right) \\ & + \frac{h^4 \pi^4}{a^4} \left(-\frac{1}{16,800} \frac{227-157\nu}{1-\nu} + \frac{1}{20} \frac{5-3\nu}{1-\nu} \bar{\zeta}^2 - \frac{1}{6} \frac{1+\nu}{1-\nu} \bar{\zeta}^4 \right) \\ & + \frac{h^6 \pi^6}{a^6} \left(\frac{1}{3,024,000} \frac{26-791\nu}{1-\nu} - \frac{1}{16,800} \frac{70-157\nu}{1-\nu} \bar{\zeta}^2 \right. \\ & \left. + \frac{1}{120} \frac{2-3\nu}{1-\nu} \bar{\zeta}^4 - \frac{1}{90} \frac{2+\nu}{1-\nu} \bar{\zeta}^6 \right) + O\left(\frac{h^8}{a^8}\right). \end{aligned} \quad (6.9)$$

Especially, we have

$$\begin{aligned}\bar{u}_3^{(P)}(0) &= 1 + \frac{1}{20} \frac{h^2 \pi^2}{a^2} \frac{8-3\nu}{1-\nu} - \frac{1}{16,800} \frac{h^4 \pi^4}{a^4} \frac{227-157\nu}{1-\nu} + \frac{1}{3,024,000} \frac{h^6 \pi^6}{a^6} \frac{26-791\nu}{1-\nu} + O\left(\frac{h^8}{a^8}\right) \\ &= 1 + 5.005299 \frac{h^2}{a^2} - 1.490127 \frac{h^4}{a^4} - 0.095966 \frac{h^6}{a^6} + O\left(\frac{h^8}{a^8}\right)\end{aligned}\tag{6.10}$$

and

$$\begin{aligned}\bar{u}_3^{(P)}(1/2) &= 1 + \frac{2}{5} \frac{h^2 \pi^2}{a^2} + \frac{27}{700} \frac{h^4 \pi^4}{a^4} - \frac{8}{23.625} \frac{h^6 \pi^6}{a^6} + O\left(\frac{h^8}{a^8}\right) \\ &= 1 + 3.947842 \frac{h^2}{a^2} + 3.757208 \frac{h^4}{a^4} - 0.325550 \frac{h^6}{a^6} + O\left(\frac{h^8}{a^8}\right)\end{aligned}\tag{6.11}$$

Equation (4.5₂) delivers

$$\begin{aligned}\bar{u}_3^{(E)}(\bar{\zeta}) &= \frac{1}{3} \sqrt{2} \frac{h^3 \pi^3}{a^3} \frac{1}{\sinh\left(\sqrt{2} \frac{h\pi}{a}\right) - \sqrt{2} \frac{h\pi}{a}} \\ &\quad \left\{ \left(\cosh\left(\sqrt{2} \frac{h\pi}{2a}\right) + \frac{\sqrt{2}}{4(1-\nu)} \frac{h\pi}{a} \sinh\left(\sqrt{2} \frac{h\pi}{2a}\right) \right) \cosh\left(\sqrt{2} \frac{h\pi}{a} \bar{\zeta}\right) \right. \\ &\quad \left. - \frac{\sqrt{2}}{1-\nu} \frac{h\pi}{2a} \bar{\zeta} \cosh\left(\sqrt{2} \frac{h\pi}{2a}\right) \sinh\left(\sqrt{2} \frac{h\pi}{a} \bar{\zeta}\right) \right\}\end{aligned}\tag{6.12}$$

with

$$\lim_{\frac{h}{a} \rightarrow 0} \bar{u}_3^{(E)}(\bar{\zeta}) = 1 = \text{const.}\tag{6.13}$$

Especially, we have

$$\bar{u}_3^{(E)}(0) = \frac{1}{3} \sqrt{2} \frac{h^3 \pi^3}{a^3} \frac{\cosh\left(\sqrt{2} \frac{h\pi}{2a}\right) + \frac{\sqrt{2}}{1-\nu} \frac{h\pi}{4a} \sinh\left(\sqrt{2} \frac{h\pi}{2a}\right)}{\sinh\left(\sqrt{2} \frac{h\pi}{a}\right) - \sqrt{2} \frac{h\pi}{a}}\tag{6.14}$$

and

$$\bar{u}_3^{(E)}(1/2) = \frac{1}{3} \sqrt{2} \frac{h^3 \pi^3}{a^3} \frac{\cosh^2\left(\sqrt{2} \frac{h\pi}{2a}\right)}{\sinh\left(\sqrt{2} \frac{h\pi}{a}\right) - \sqrt{2} \frac{h\pi}{a}}\tag{6.15}$$

A comparison for the transverse displacement \bar{u}_3 at the centre ($\bar{\zeta} = 0$) and at the faces $\bar{\zeta} = \pm \frac{1}{2}$ of the plate is given in Table 2 for different values of $\frac{h}{a}$.

Table 2. Values for the displacements \bar{u}_3

| $\frac{h}{a}$ | 0 | $\frac{1}{10}$ | $\frac{1}{5}$ | $\frac{1}{3}$ | $\frac{1}{2}$ |
|----------------------------|---|----------------|---------------|---------------|---------------|
| $\bar{u}_3^{(P)}(0)$ | 1 | 1.0499 | 1.1978 | 1.5376 | 2.1567 |
| $\bar{u}_3^{(E)}(0)$ | 1 | 1.0499 | 1.1978 | 1.5377 | 2.1575 |
| $\Delta\%$ | 0 | 0.00 | 0.00 | 0,01 | 0.04 |
| $\bar{u}_3^{(P)}(\pm 1/2)$ | 1 | ± 1.0399 | ± 1.1639 | ± 1.4846 | ± 2.2167 |
| $\bar{u}_3^{(E)}(\pm 1/2)$ | 1 | ± 1.0399 | ± 1.1639 | ± 1.4846 | ± 2.2165 |
| $\Delta\%$ | 0 | 0.00 | 0.00 | 0.00 | 0.01 |

We see that the values of the second-order consistent plate theory and the three-dimensional theory of elasticity are in excellent agreement with each other even for ratios $h/a = 1/2$ which are rather solid bricks than plates.

Fig. 8 shows the distribution of $\bar{u}_3^{(E)}\left(\bar{\zeta}, \frac{h}{a}\right)$ along the plate thickness. The deviation from the classical assumption of the thin-plate theory $\bar{u}_3 = \text{const.} \neq f(\bar{\zeta})$ becomes visible with 5% already for relatively thin plates of $h/a = 1/10$ and increase considerably for thicker plates. The differences between the elasticity and plate solutions are less than 1‰. Both solutions are plotted in Fig. 9 for $h/a = 1/3$. Differences are not visible in the plot, the maximal difference occurs at $\bar{\zeta} = 0$. (cf. Table 2). Fig. 10 shows the development of $\bar{u}_3^{(P)}\left(\bar{\zeta}, \frac{1}{3}\right)$ for different approximation orders. Considering (6.9), we define

$$\begin{aligned}
\bar{u}_3^0\left(\bar{\zeta}, \frac{h}{a}\right) &= 1, \\
\bar{u}_3^1\left(\bar{\zeta}, \frac{h}{a}\right) &= 1 + \frac{h^2 \pi^2}{a^2} \left(\frac{1}{20} \frac{8-3\nu}{1-\nu} - \frac{\nu}{1-\nu} \bar{\zeta}^2 \right), \\
\bar{u}_3^2\left(\bar{\zeta}, \frac{h}{a}\right) &= 1 + \frac{h^2 \pi^2}{a^2} \left(\frac{1}{20} \frac{8-3\nu}{1-\nu} - \frac{\nu}{1-\nu} \bar{\zeta}^2 \right) \\
&\quad + \frac{h^4 \pi^4}{a^4} \left(-\frac{1}{16.800} \frac{227-157\nu}{1-\nu} + \frac{1}{20} \frac{5-3\nu}{1-\nu} \bar{\zeta}^2 - \frac{1}{6} \frac{1+\nu}{1-\nu} \bar{\zeta}^4 \right), \\
\bar{u}_3^3\left(\bar{\zeta}, \frac{h}{a}\right) &= \bar{u}_3^{(P)}\left(\bar{\zeta}, \frac{h}{a}\right) \triangleq (6.9).
\end{aligned} \tag{6.16}$$

The transverse displacement \bar{u}_3^0 represents the result of the classical theory and is equal to $1 = \text{const}$. The first order approximation (quadratic parabola) improves the solution considerably, whereas the second-order approximation adjusts the displacement in a still visible manner. The third-order term, which is not fully fixed within a consistent second-order plate theory, results in marginal improvements not visible in Fig. 10.

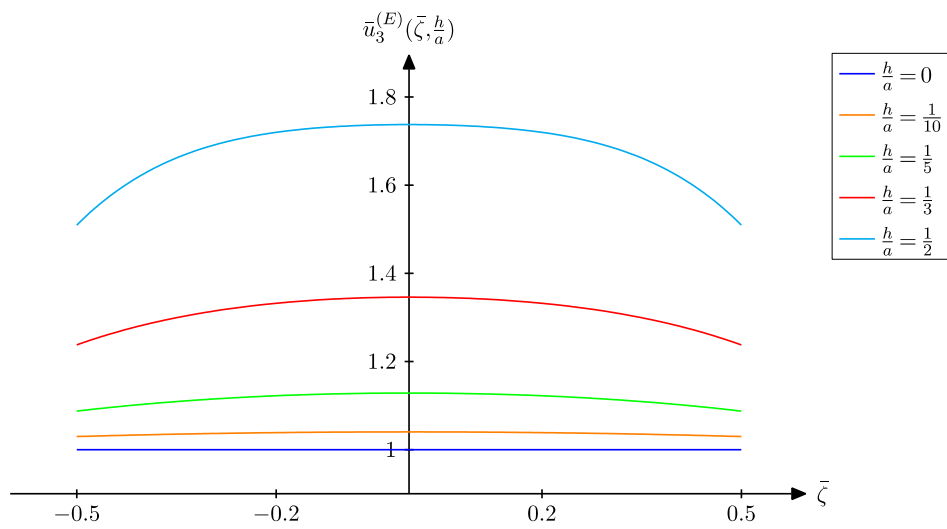


Fig. 8. Transverse displacement ${}^3u^{(E)}\left(\bar{\zeta}, \frac{h}{a}\right)$ along the plate thickness with $\frac{h}{a}$ as parameter

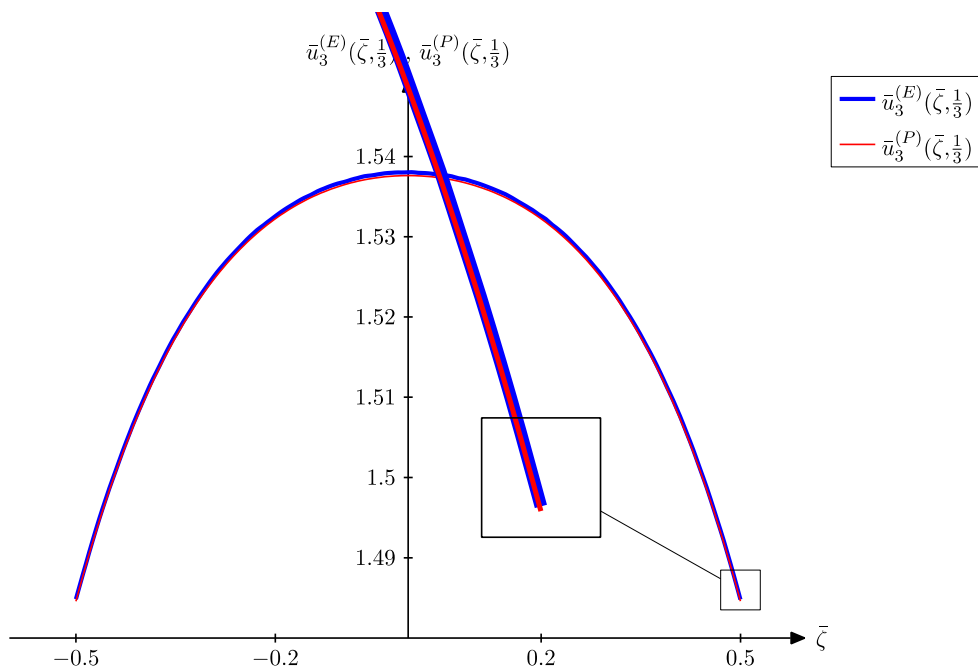


Fig. 9. Comparison of the exact elasticity solution $\bar{u}_1^{(E)}$ and the second-order consistent plate-theory solution $\bar{u}_3^{(P)}$ along the non-dimensionalised thickness coordinate $\bar{\zeta}$ for $h/a = 1/3$

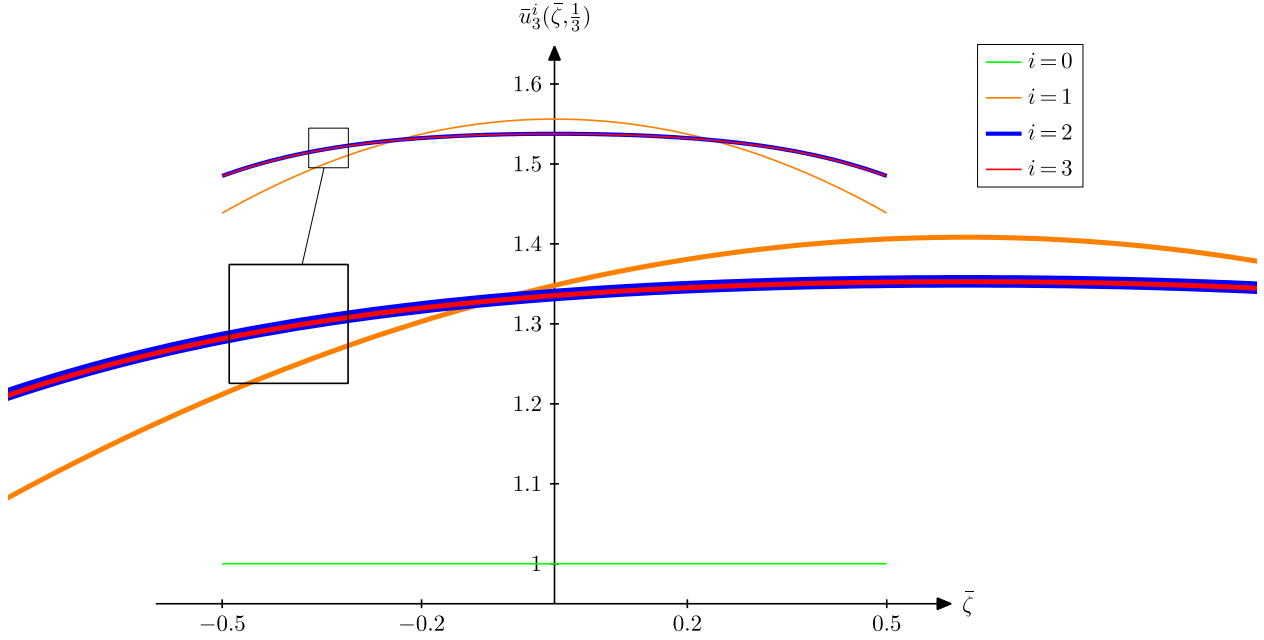


Fig. 10. Transverse displacement \bar{u}_3^i for different approximation orders

Proceeding further to the stresses, we introduce

$$\bar{\sigma}_{11}(\bar{\zeta}) = \bar{\sigma}_{22}(\bar{\zeta}) = \frac{2\pi^2}{3(1+\nu)} \frac{h^2}{a^2 P_0} \sigma_{11}\left(\frac{1}{2}, \frac{1}{2}, \bar{\zeta}\right) = \frac{2\pi^2}{3(1+\nu)} \frac{h^2}{a^2 P_0} \sigma_{22}\left(\frac{1}{2}, \frac{1}{2}, \bar{\zeta}\right) \quad (6.17)$$

and find

$$\begin{aligned} \bar{\sigma}_{11}^{(P)}(\bar{\zeta}) &= \bar{\sigma}_{22}^{(P)}(\bar{\zeta}) \\ &= 2\bar{\zeta} \left\{ 1 - \frac{h^2 \pi^2}{a^2} \left(\frac{1}{20} \frac{2-3\nu}{1+\nu} - \frac{1}{3} \frac{2+\nu}{1+\nu} \bar{\zeta}^2 \right) \right. \\ &\quad \left. + \frac{h^4 \pi^4}{a^4} \left(-\frac{1}{16,800} \frac{87+157\nu}{1+\nu} + \frac{1}{60} \frac{1+3\nu}{1+\nu} \bar{\zeta}^2 + \frac{1}{30} \frac{3+\nu}{1+\nu} \bar{\zeta}^4 \right) + O\left(\frac{h^6}{a^6}\right) \right\}. \end{aligned} \quad (6.18)$$

Especially at the plate faces we have

$$\begin{aligned}\bar{\sigma}_{11}^{(P)}(\pm 1/2) &= \pm \left(1 + \frac{h^2 \pi^2}{a^2} \frac{1}{30} \frac{2+7\nu}{1+\nu} + \frac{h^4 \pi^4}{a^4} \frac{11}{2,100} \right) \\ &= \pm \left(1 + \frac{h^2}{a^2} 1.037574 + \frac{h^4}{a^4} 0.510238 \right).\end{aligned}\quad (6.19)$$

The elasticity solution follows from (4.6₁) as

$$\begin{aligned}\bar{\sigma}_{11}^{(E)}(\bar{\zeta}) &= \sigma_{22}^{(E)}(\bar{\zeta}) = \frac{1}{3} \frac{1}{1+\nu} \frac{h^2 \pi^2}{a^2} \cdot \frac{1}{\sinh\left(\sqrt{2} \frac{h\pi}{a}\right) - \sqrt{2} \frac{h\pi}{a}} \\ &\quad \left\{ (1+2\nu) \cosh\left(\sqrt{2} \frac{h\pi}{2a}\right) \sinh\left(\sqrt{2} \frac{h\pi}{a} \bar{\zeta}\right) \right. \\ &\quad \left. + \sqrt{2}\pi \left(\frac{h}{a} \bar{\zeta} \cosh\left(\sqrt{2} \frac{h\pi}{2a}\right) \cosh\left(\sqrt{2} \frac{h\pi}{a} \bar{\zeta}\right) - \frac{h}{2a} \sinh\left(\sqrt{2} \frac{h\pi}{2a}\right) \sinh\left(\sqrt{2} \frac{h\pi}{a} \bar{\zeta}\right) \right) \right\}\end{aligned}\quad (6.20)$$

with

$$\lim_{\frac{h}{a} \rightarrow 0} \bar{\sigma}_{11}^{(E)}(\bar{\zeta}) = 2\bar{\zeta}.\quad (6.21)$$

Especially, for $\bar{\zeta} = \pm \frac{1}{2}$ we find

$$\bar{\sigma}_{11}^{(E)}(\pm 1/2) = \pm \frac{1}{6} \frac{1}{1+\nu} \frac{h^2 \pi^2}{a^2} \frac{(1+2\nu) \sinh\left(\sqrt{2} \frac{h\pi}{a}\right) + \sqrt{2} \frac{h\pi}{a}}{\sinh\left(\sqrt{2} \frac{h\pi}{a}\right) - \sqrt{2} \frac{h\pi}{a}}.\quad (6.22)$$

The normal stresses for the plate faces taken from (6.19) and (6.22) are compiled in Table 3.

Table 3. Non-dimensional normal stresses $\bar{\sigma}_{11}$ and $\bar{\sigma}_{22}$ at the plate faces $\bar{\zeta} = \pm 1/2$

| $\frac{h}{a}$ | 0 | $\frac{1}{10}$ | $\frac{1}{5}$ | $\frac{1}{3}$ | $\frac{1}{2}$ |
|------------------------------------|---------|----------------|---------------|---------------|---------------|
| $\bar{\sigma}_{11}^{(P)}(\pm 1/2)$ | ± 1 | ± 1.0104 | ± 1.0423 | ± 1.1216 | ± 1.2913 |
| $\bar{\sigma}_{11}^{(E)}(\pm 1/2)$ | ± 1 | ± 1.0104 | ± 1.0423 | ± 1.1214 | ± 1.2887 |
| $\Delta \%$ | 0 | 0.00 | 0.00 | 0.02 | 0.20 |

In Fig. 11, the bending-stress distribution over the plate thickness is depicted. The deviation from the classical linear distribution becomes visible for $h/a > 1/5$ and gets more pronounced for larger values. The distributions of the exact elasticity solution and the second-order plate theory practically coincide (cf. Fig. 12). The main difference occurs at $\bar{\zeta} = \pm 1/2$ (cf. Table 3). Again, we discuss the influence of the approximation order on the stress distributions. In view of (6.18), we introduce

$$\begin{aligned}\bar{\sigma}_{11}^1\left(\bar{\zeta}, \frac{h}{a}\right) &= 2\bar{\zeta} \\ \bar{\sigma}_{11}^2\left(\bar{\zeta}, \frac{h}{a}\right) &= 2\bar{\zeta}\left(1 - \frac{h^2\pi^2}{a^2}\left(\frac{1}{20}\frac{2-3\nu}{1+\nu} - \frac{1}{3}\frac{2+\nu}{1+\nu}\bar{\zeta}^2\right)\right) \\ \bar{\sigma}_{11}^3\left(\bar{\zeta}, \frac{h}{a}\right) &= \bar{\sigma}_{11}(\bar{\zeta}) \hat{=} (6.18)\end{aligned}\tag{6.23}$$

and plot the results in Fig. 13. The stress distribution given by $\bar{\sigma}_{11}^1$ coincides with classical linear assumption, $\bar{\sigma}_{11}^2$ represents the correction within the consistent second-order theory. Terms from the third-order theory supply only marginal changes.

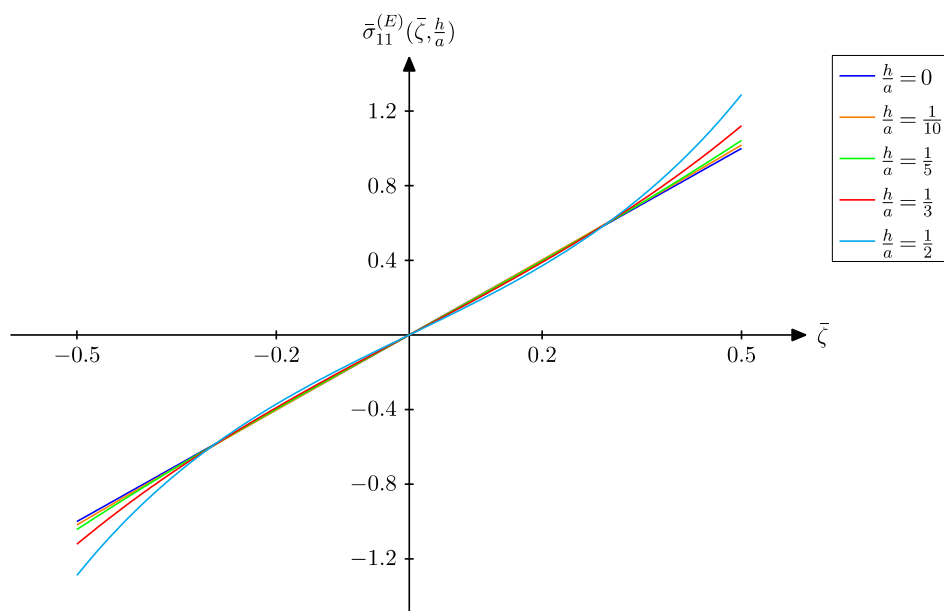


Fig. 11. Distribution of $\bar{\sigma}_{11}^{(E)}\left(\bar{\zeta}, \frac{h}{a}\right)$ along the plate thickness with h/a as parameter

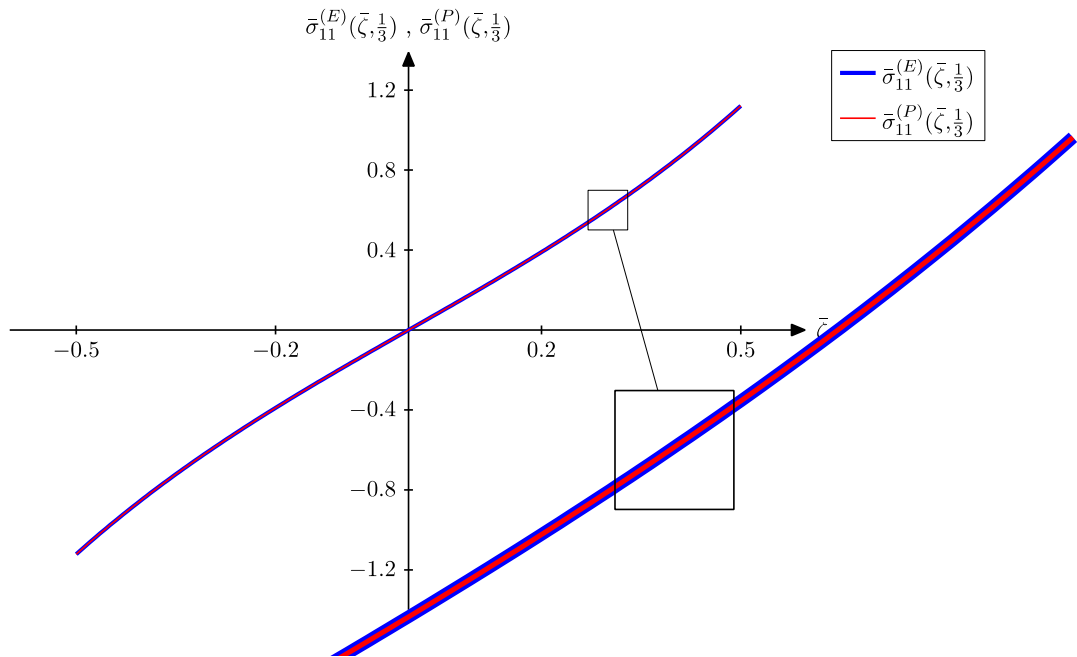


Fig. 12. Comparison of the exact elasticity solution $\bar{\sigma}_{11}^{(E)}$ and the second order plate theory $\bar{\sigma}_{11}^{(P)}$ along the non-dimensionalised thickness coordinate $\bar{\zeta}$ for $h/a = 1/3$

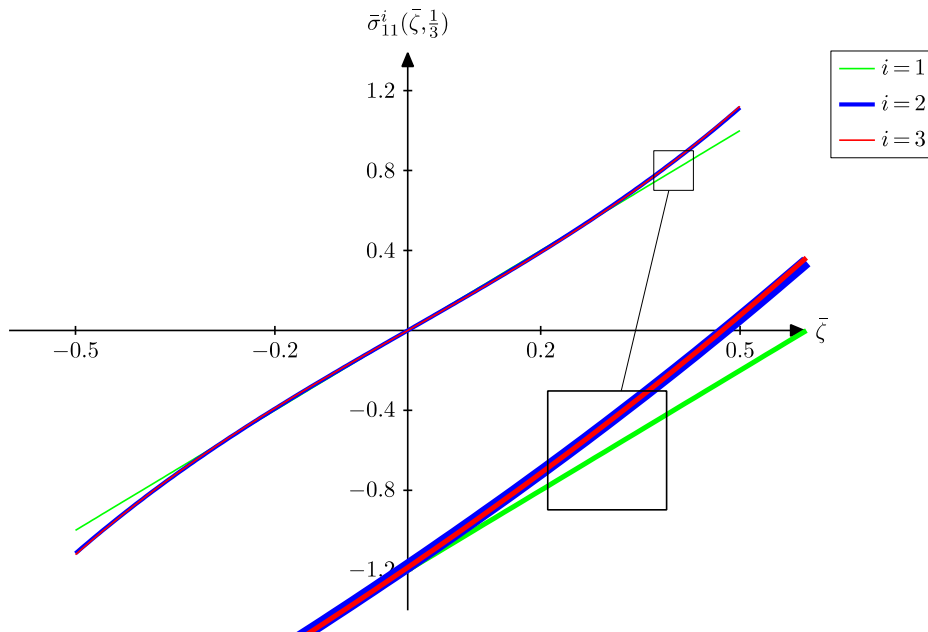


Fig. 13. Bending stress $\bar{\sigma}_{11}^i$ for different approximation orders

Similar results and conclusion are valid for the in-plane shear stresses σ_{12} , the results for which will be omitted here.

For the transverse shear stresses, we introduce

$$\bar{\sigma}_{13}(\bar{\zeta}) = \frac{4\pi}{3} \frac{h}{aP_0} \sigma_{13} \left(0, \frac{1}{2}, \bar{\zeta} \right) = \frac{4\pi}{3} \frac{h}{aP_0} \sigma_{23} \left(\frac{1}{2}, 0, \bar{\zeta} \right) \quad (6.24)$$

and find with (3.84)

$$\bar{\sigma}_{13}^{(P)}(\bar{\zeta}) = \bar{\sigma}_{23}^{(P)}(\bar{\zeta}) = (1 - 4\bar{\zeta}^2) \left(1 - \frac{h^2 \pi^2}{a^2} \frac{1}{60} (1 - 20\bar{\zeta}^2) + O\left(\frac{h^4}{a^4}\right) \right). \quad (6.25)$$

Especially at the plate middle surface $\bar{\zeta} = 0$, we have

$$\bar{\sigma}_{13}^{(P)}(0) = 1 - \frac{h^2 \pi^2}{a^2} \frac{1}{60} = 1 - 0.164493 \frac{h^2}{a^2}. \quad (6.26)$$

The elasticity solutions turns out to be (4.6₃)

$$\bar{\sigma}_{13}^{(E)}(\bar{\zeta}) = \frac{2}{3} \frac{h^2 \pi^2}{a^2} \frac{\sinh\left(\sqrt{2} \frac{h\pi}{2a}\right) \cosh\left(\sqrt{2} \frac{h\pi}{a} \bar{\zeta}\right) - 2\bar{\zeta} \cosh\left(\sqrt{2} \frac{h\pi}{a}\right) \sinh\left(\sqrt{2} \frac{h\pi}{a} \bar{\zeta}\right)}{\sinh\left(\sqrt{2} \frac{h\pi}{a}\right) - \sqrt{2} \frac{h\pi}{a}} \quad (6.27)$$

with

$$\lim_{\frac{h}{a} \rightarrow 0} \bar{\sigma}_{13}^{(E)}(\bar{\zeta}) = 1 - 4\bar{\zeta}^2.$$

Especially at the plate middle surface, we find

$$\bar{\sigma}_{13}^{(E)}(0) = \frac{2}{3} \frac{h^2 \pi^2}{a^2} \frac{\sinh\left(\sqrt{2} \frac{h\pi}{2a}\right)}{\sinh\left(\sqrt{2} \frac{h\pi}{a}\right) - \sqrt{2} \frac{h\pi}{a}}. \quad (6.28)$$

Numerical values are given in Table 5.

Table 5. Non-dimensionalised transverse shear stresses $\bar{\sigma}_{13}$ and $\bar{\sigma}_{23}$ at the plate middle surface $\bar{\zeta} = 0$

| $\frac{h}{a}$ | 0 | $\frac{1}{10}$ | $\frac{1}{5}$ | $\frac{1}{3}$ | $\frac{1}{2}$ |
|------------------------------|---|----------------|---------------|---------------|---------------|
| $\bar{\sigma}_{13}^{(P)}(0)$ | 1 | 0.9984 | 0.9934 | 0.9817 | 0.9589 |
| $\bar{\sigma}_{13}^{(E)}(0)$ | 1 | 0.9983 | 0.9933 | 0.9806 | 0.9537 |
| $\Delta\%$ | 0 | 0.01 | 0.01 | 0.11 | 0.54 |

Although the approximation order is less than for $\bar{\sigma}_{\alpha\beta}$, the agreement between both solutions is again excellent.

As depicted in Fig. 16, the classical quadratic transverse-shear distribution (Dübelformel) occurs for $h/a \rightarrow 0$, and is slightly changed to a bi-quadratic solution within the second-order plate theory.

The differences between the exact elasticity solution and the second-order plate theory are less than 1% and are not visible in Fig. 17 for $h/a = 1/3$. The maximal derivation occurs at $\bar{\zeta} = 0$, cf. Table 5.

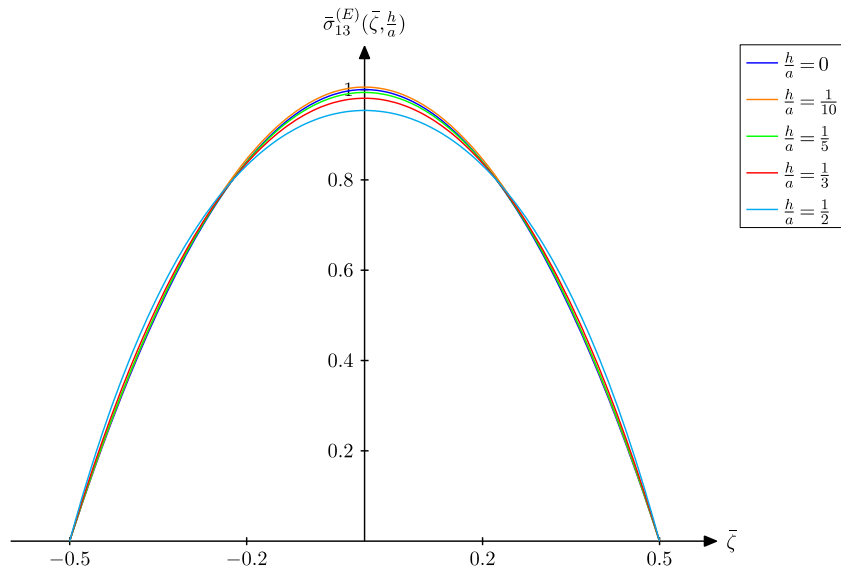


Fig. 16. Transverse-shear distribution $\bar{\sigma}_{13}\left(\bar{\zeta}, \frac{h}{a}\right)$ along the plate thickness with h/a as parameter

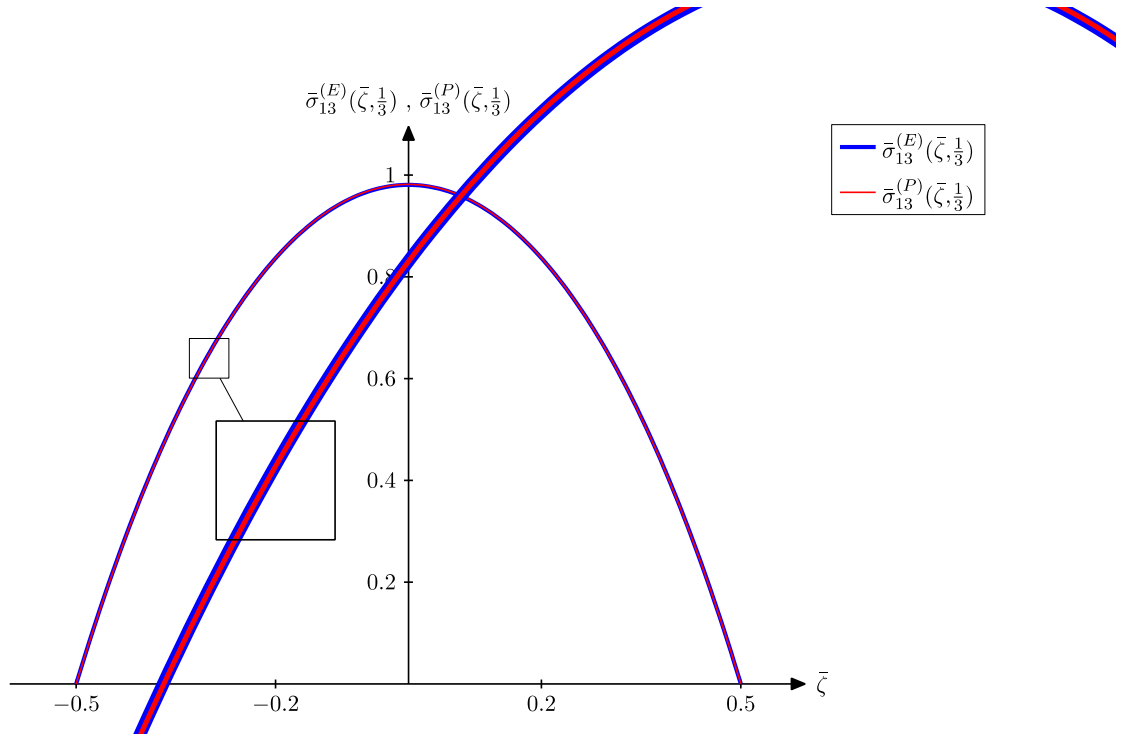


Fig. 17. Comparison of the exact elasticity solution $\bar{\sigma}_{13}^{(E)}$ and the second-order plate theory $\bar{\sigma}_{13}^{(P)}$ along the non-dimensionalized thickness coordinate $\bar{\zeta}$ for $h/a = 1/3$

Finally, we investigate the transverse normal stresses σ_{33} and introduce

$$\bar{\sigma}_{33}(\bar{\zeta}) = \frac{1}{P_0} \sigma_{33} \left(\frac{1}{2}, \frac{1}{2}, \bar{\zeta} \right) \quad (6.29)$$

and find for the plate solution, cf. (3.8₆)

$$\bar{\sigma}_{33}^{(P)}(\bar{\zeta}) = \bar{\zeta} \left(\frac{1}{2} (3 - 4\bar{\zeta}^2) - \frac{h^2 \pi^2}{a^2} \frac{1}{40} (1 - 8\bar{\zeta}^2 + 16\bar{\zeta}^4) + O\left(\frac{h^4}{a^4}\right) \right). \quad (6.30)$$

$\bar{\sigma}_{33}^{(P)}$ at $\bar{\zeta} = 0$ is zero and at $\bar{\zeta} = \pm \frac{1}{2}$ it is $\pm \frac{1}{2}$ as prescribed by the boundary conditions.

For comparison, we evaluate σ_{33} at $\bar{\zeta} = \frac{1}{4}$ and find

$$\bar{\sigma}_{33}^{(P)}(1/4) = \frac{11}{32} - \frac{h^2 \pi^2}{a^2} \frac{9}{640} = 0.343750 - 0.138791 \frac{h^2}{a^2}. \quad (6.31)$$

The elasticity solution turns out to be (4.64)

$$\begin{aligned} \bar{\sigma}_{33}^{(E)}(\bar{\zeta}) = & \frac{1}{\sinh\left(\sqrt{2}\frac{h\pi}{a}\right) - \sqrt{2}\frac{h\pi}{a}} \cdot \left\{ \cosh\left(\sqrt{2}\frac{h\pi}{2a}\right) \sinh\left(\sqrt{2}\frac{h\pi}{a}\bar{\zeta}\right) \right. \\ & \left. + \sqrt{2}\frac{h\pi}{2a} \left(\sinh\left(\sqrt{2}\frac{h\pi}{2a}\right) \sinh\left(\sqrt{2}\frac{h\pi}{a}\bar{\zeta}\right) - 2\bar{\zeta} \cosh\left(\sqrt{2}\frac{h\pi}{2a}\right) \cosh\left(\sqrt{2}\frac{h\pi}{a}\bar{\zeta}\right) \right) \right\} \end{aligned} \quad (6.32)$$

with

$$\lim_{\frac{h}{a} \rightarrow 0} \bar{\sigma}_{33}^{(E)}(\bar{\zeta}) = \frac{1}{2} \bar{\zeta} (3 - 4\bar{\zeta}^2). \quad (6.33)$$

In Table 6, the values of $\bar{\sigma}_{33}(1/4)$ from (6.31) and (6.32) are compared and, again, an excellent agreement is observed.

Table 6. Transverse normal stresses $\bar{\sigma}_{33}$ evaluated at $\bar{\zeta} = 1/4$

| $\frac{h}{a}$ | 0 | $\frac{1}{10}$ | $\frac{1}{5}$ | $\frac{1}{3}$ | $\frac{1}{2}$ |
|--------------------------------|--------|----------------|---------------|---------------|---------------|
| $\bar{\sigma}_{33}^{(P)}(1/4)$ | 0.3438 | 0.3434 | 0.3425 | 0.3399 | 0.3351 |
| $\bar{\sigma}_{33}^{(E)}(1/4)$ | 0.3438 | 0.3434 | 0.3423 | 0.3396 | 0.3339 |
| $\Delta \%$ | 0 | 0.00 | 0.06 | 0.09 | 0.36 |

As can be seen in Figs. 18 and 19, the through-thickness distribution of $\bar{\sigma}_{33}^{(E)}\left(\bar{\zeta}, \frac{h}{a}\right)$ is hardly influenced by the relative thickness h/a of the plate. The maximal difference between the exact elasticity solution and the second-order plate solution occurs at $\bar{\zeta} = \pm 0.236 \cong 1/4$, cf. Table 6.

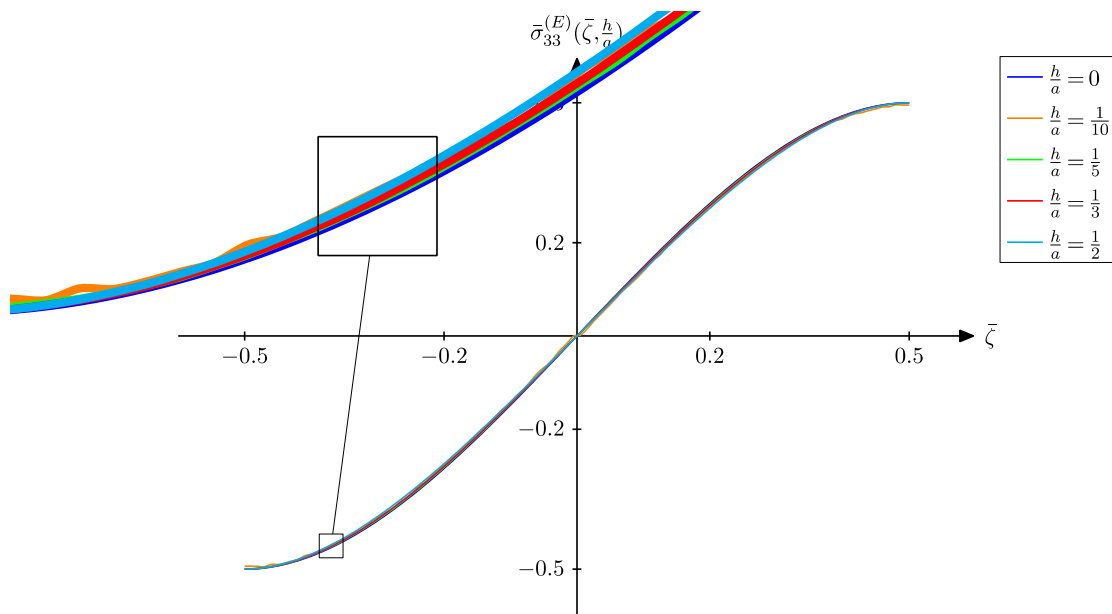


Fig. 18. Transverse normal stress $\bar{\sigma}_{33}^{(E)}\left(\bar{\zeta}, \frac{h}{a}\right)$ along the plate thickness with h/a as parameter

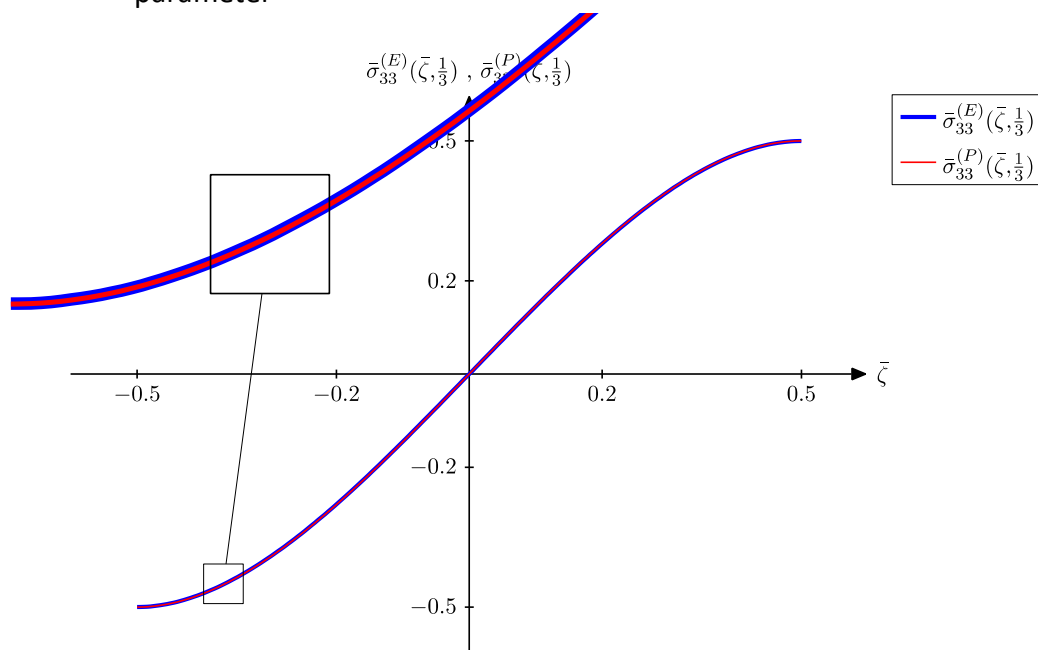


Fig. 19. Comparison of the exact elasticity solution $\bar{\sigma}_{33}^{(E)}$ and the second-order plate theory $\bar{\sigma}_{33}^{(P)}$ along the non-dimensionalised thickness coordinate $\bar{\zeta}$ for $h/a = 1/3$

7. Conclusions

For the simply supported rectangular plate under sinusoidal load, closed form solutions are available within the consistent second-order plate theory as well as within the three-dimensional theory of elasticity. A Taylor-series expansion of the exact elasticity solution with respect to the non-dimensionalised thickness h/a reveals that the formulae of the plate theory coincide exactly with the first terms of the Taylor-series expansion. We were able to identify two constants which had not been determined within the second-order consistent plate theory.

For both theories, maximal values for displacements and stresses are evaluated for the special case of a quadratic plate under a single-waved load ($m = n = \alpha = 1$). The values of both theories show a remarkably good agreement. Even for thick plates with $h/a = 1/2$ - which are rather three-dimensional bricks than plates - the deviation turns out to be far less than 1%.

In a forthcoming paper we will treat transversely isotropic plates and show that the arguments may be applied equally well.

8. Acknowledgements

Financial support of this research by The Royal Society (UK) International Exchanges award (IE161021) is gratefully acknowledged.

9. References

- Altenbach, H., Altenbach, J., Eremeyev, V. (2010) On generalized Cosserat-type theories of plates and shells: A short review and bibliography. *Arch. Appl. Mech.* 80: 73-92
- Brischetto, S. (2017) Exact three-dimensional static analysis of single- and multi-layered plates and shells. *Composites Part B: Engineering*, 119: 230-252
- Bronstein, I. N., Semendjajew, K. A. (1996) *Taschenbuch der Mathematik*, Teubner, Stuttgart, 1996
- Candiotti, S., Mantari, J.L., Yarasca, J., Petrolo, M., E. Carrera, E. (2017) An axiomatic/asymptotic evaluation of best theories for isotropic metallic and functionally graded plates employing non-polynomic functions. *Aerospace Sci. and Tech.* 68: 179-192
- Friesecke, G., James, R. D., Müller, S. (2002a) A theorem on geometric rigidity and the derivation of nonlinear plate theory from three-dimensional elasticity. *Commun. Pure Appl. Math* 55: 1461-1506
- Friesecke, G., Müller, S., James, R. D. (2002b) Rigorous derivation of nonlinear plate theory and geometric rigidity. *Comptes Rendus Math.* 334: 173-178
- Giorgi, E. D. (1975) Sulla convergenza di alcune successioni di integrali del tipo dell'aera. *Rend. Mat. Appl.* 8: 277-294
- Karttunen, A.T., Herten, R., Reddy, J.N., Jani Romanoff, J. (2017) Bridging plate theories and elasticity solutions. *Int. J. Solids and Struct.* 106–107: 251-263
- Kienzler, R. (1982) Eine Erweiterung der klassischen Schalentheorie; Der Einfluss von Dickenverzerrungen und Querschnittsverwölbungen. *Ing. Arch.* 52: 311-322. Extended version in: PhD Thesis, Technische Hochschule Darmstadt, Darmstadt (1980)
- Kienzler, R. (2002) On consistent plate theories. *Arch. Appl. Mech.* 72: 229-247
- Kienzler, R.: (2004) On consistent second-order plate theories. In: Kienzler, R., Altenbach, H., Ott, I. (Eds.) *Theories of plates and shells: critical review and new applications*. Springer, Berlin: 85-96
- Kienzler, R., Schneider, P. (2012) Consistent theories of isotropic and anisotropic plates. *J. Theoret. Appl. Mech.* 50: 755-768
- Kienzler, R., Schneider, P. (2017) Second-order linear plate theories: Partial differential equations, stress resultants and displacements. *Int. J. Solids and Struct.* 115-116: 14-26
- Koiter, W. (1966) On the nonlinear theory of thin elastic shells. *Koninklijke Nederlandse Akademie van Wetenschappen, Proceedings, Series B* 69: 1-54
- Koiter, W. (1970a) On the foundation of the linear theory of thin elastic shells. *Koninklijke Nederlandse Akademie van Wetenschappen, Proceedings, Series B* 73: 169-195
- Koiter, W. (1970b) On the mathematical foundation of shell theory. In: *Proc. Int. Congr. Math., Nice* 3: 123-130
- Krätzig, W. (1980) On the structure of consistent linear shell theories. In: Koiter, W., Mikhailov, G. (Eds.). *Theory of Plates and Shells*: 353-368. North-Holland, Amsterdam
- Naghdi, P. M. (1963) Foundations of elastic shell theory. In: Sneddon, I, Hill, R. (Eds.) *Progress in Solid Mechanics* 4, North-Holland, Amsterdam: 1-90.
- Pruchnicki, E. (2014) Two-dimensional model of order h^5 for the combined bending, stretching, transverse shearing and transverse normal stress effects of homogeneous plates derived from three-dimensional elasticity. *Math. Mech. Solids* 19: 477-490

- Repka, M., Sladek, V., Sladek, J. (2018) Gradient elasticity theory enrichment of plate bending theories. *Comp. Struct.* 202: 447-457
- Reddy, J. N. (1984) A refined nonlinear theory of plates with transverse shear deformation. *Int. J. Solids Struct.* 22: 881-896
- Reissner, E. (1944) On the theory of bending of elastic plates. *J. Math. Phys.* 23: 184-191
- Reissner, E. (1945) On the effect of transverse shear deformation on the bending of elastic plates. *J. Appl. Mech.* 12: 69-77
- Saidi, A. R., Atashipour, S. R., Jomehzadeh, E. (2009) Reformulation of Navier equations for solving three-dimensional elasticity problems with applications to thick plate analysis. *Acta Mech.* 208: 227-235
- Schneider, P., Kienzler, R. (2011) An algorithm for the automatization of pseudo reductions of PDE systems arising from the uniform-approximation technique. In: Altenbach H., Eremeyew, V. A. (Eds.). *Shell-like structures: Non-Classical Theories and Applications. Advanced Structural Materials 15.* Springer, Berlin: 377-390
- Schneider, P., Kienzler, R. (2015a) On exact rod/beam/shaft theories and the coupling among them due to arbitrary material anisotropies. *Int. J. Solids Struct.* 56-57: 265-279
- Schneider, P., Kienzler, R. (2015b) Comparison of various linear plate theories in the light of a consistent second-order approximation. *Math. Mech. Sol.* 20: 871-882
- Schneider, P., Kienzler, R. (2017) A Reissner-type plate theory for monoclinic material derived by extending the uniform-approximation technique by orthogonal tensor decompositions of n th-order gradients. *Mechanica* 52: 2143-2167
- Schneider, P., Kienzler, R. (2019) A priori estimation of the systematic error of consistently derived theories for thin structures. Submitted
- Schneider, P., Kienzler, R., Böhm, M. (2014) Modelling of consistent second-order plate theories for anisotropic materials. *Z. Angew. Math. Mech.* 94: 21-42
- Steigmann, D. J. (2008) Two-dimensional models for the combined bending and stretching of plates and shells based on three-dimensional linear elasticity. *Int. J. Engng. Sci.* 46: 654-676
- Steigmann, D. J. (2012) Refined theory of linear elastic plates: Laminae and laminates. *Math. Mech. Solids* 17: 351-363
- Szabo, I. (1987) *Geschichte der mechanischen Prinzipien.* Birkhäuser, Basel
- Vekua, I. (1955) On one method to calculating prismatic shells (In Russian). *Trudy Tbilisi. Mat. Inst.* 21: 191-259
- Vekua, I. (1985) *Shell theory: general methods of construction.* Monographs, Advanced Texts and Surveys in Pure and Applied Mathematics. John Wiley & Sons, New York
- Wang, F.F., Steigmann, D.J., Dai, H.H. (2019) On a uniformly-valid asymptotic plate theory. *Int. J. of Non-Linear Mech.*, in press
- Wang, C. M., Reddy, J. N., Lee, K. H. (2000) *Shear deformable beams and plates.* Elsevier, Amsterdam
- Youngdahl, C.K. (1969) On the completeness of a set of stress functions appropriate to the solutions of elasticity problems in general cylindrical co-ordinates. *Int. J. Eng. Sci.* 7: 61-79.